UPPSALA
UNIVERSITET

Digital Comprehensive Summaries of Uppsala Dissertations from the Faculty of Science and Technology 142

Studies of the Reactive Sputtering Process and its Application in Electro-Acoustic Devices

DANIEL ROSÉN

ACTA
UNIVERSITATIS
UPSALIENSIS
UPPSALA
2006

ISSN 1651-6214
ISBN 91-554-6452-1
urn:nbn:se:uu:diva-6320

Dissertation presented at Uppsala University to be publicly examined in 10134, Ångström Laboratory, Friday, February 17, 2006 at 10:00 for the degree of Doctor of Philosophy. The examination will be conducted in English.

Abstract
Rosén, D. 2006. Studies of the Reactive Sputtering Process and its Application in Electro-Acoustic Devices. Acta Universitatis Upsaliensis. *Digital Comprehensive Summaries of Uppsala Dissertations from the Faculty of Science and Technology* 142. 61 pp. Uppsala. ISBN 91-554-6452-1.

Electro-acoustic devices such as surface acoustic wave (SAW) and bulk acoustic wave (BAW) devices have been in commercial use for over 60 years and can be found in applications ranging from specialised scientific and military equipment to consumer products, such as mobile telephones, TV and radio receivers, etc. Today by far the largest market for electro-acoustic devices is the telecommunication industry which annually consumes approximately three billion acoustic wave filters for frequency control alone.

The development of new materials and technologies for electro-acoustic devices has gained a substantial and growing interest from both academic and industrial research communities in recent years due to the enormous growth in the telecommunication industry and other forms of wireless data communication. One of the bigger issues has been to replace the single crystalline substrates with thin film piezoelectric materials deposited by reactive sputtering. This would not only reduce the manufacturing costs but will also enable high frequency of operation and a wider choice of substrate materials. However, in order to obtain the material properties required for the intended application a detailed theoretical description of the reactive sputtering process is necessary since the texture and other functional properties of the piezoelectric material are extremely sensitive to the process parameters in addition to the structure of the underlying material.

This thesis studies the reactive sputtering process and its application for the fabrication of thin film electro-acoustic devices. The aim has been to gain a further insight into the process and make use of this knowledge to improve the fabrication of electro-acoustic devices. In this work modelling of the reactive sputtering process has been improved by studying certain fundamental aspects of the process and in particular the dynamics of the processes taking place during sputtering both at the target and the substrate surfaces. Consequently, highly textured thin piezoelectric aluminium nitride films have been synthesized and thin film bulk acoustic resonators (FBAR) operating in the GHz range have been fabricated and studied.

Keywords: Sputtering, Reactive Sputtering, Electro Acoustic Devices

Daniel Rosén, Department of Engineering Sciences, Solid State Electronics, Box 534, Uppsala University, SE-75121 Uppsala, Sweden

© Daniel Rosén 2006

ISSN 1651-6214
ISBN 91-554-6452-1
urn:nbn:se:uu:diva-6320 (http://urn.kb.se/resolve?urn=urn:nbn:se:uu:diva-6320)

List of Publications

I TRIDYN Simulation of Target Poisoning in Reactive Sputtering
D. Rosén, I. Katardjiev, S. Berg, and W. Möller
Nucl. Instr. and Meth. B, vol. **228**, pp. 193-197, 2005

II Suppression of Spurious Lateral Modes in Thickness-Excited FBAR Resonators
D. Rosén, J. Bjurström, and I. Katardjiev
IEEE Trans. Ultrason. Ferroelect. Freq. Contr., vol. **52**(7), pp. 1189-1192, 2005

III Dependence of the Electromechanical Coupling on the Degree of Orientation of C-Textured Thin AlN Films
J. Bjurström, D. Rosén, I. Katardjiev, V.M. Yanchev, and I. Petrov
IEEE Trans. Ultrason. Ferroelect. Freq. Contr., vol. **51**(10), pp. 1347-1353, 2004

IV Defining the Surface Binding Energy in Dynamic Monte Carlo Simulation for Reactive Sputtering of Compounds
D. Rosén
To be published in Vacuum

V Aluminium Nitride Deposition on 4H-SiC by Means of Physical Vapour Deposition
M. Wolborski, D. Rosén, A. Hallén, and M. Bakowski
Submitted to Thin Solid Films

VI Modelling of Sputter Erosion Rate Enhancement from Ceramic Targets
T. Nyberg, O. Kappertz, D. Rosén, T. Kubart, D. Severin, A. Pflug, and S. Berg
Proceedings to Society of Vacuum Coaters, pp. 324-328, 2004

VII Influence of Rotating Magnets on Hysteresis in Reactive Sputtering
O. Kappertz, T. Nyberg, D. Rosén, and S. Berg
Proceedings to Society of Vacuum Coaters, pp. 271-275, 2004

VIII Dynamic Behaviour of Metallic Targets in Reactive Sputtering
D. Rosén, I. Katardjiev, and S. Berg
Manuscript

Related Publications

I Membrane Covered Electrically Isolated Through-Wafer Via Holes
D. Rosén, J. Olsson, and C. Hedlund
J. Micromech. Microeng., vol. **11**(4), pp. 344-347, 2001

II Innovative Process Development for a New Micro-Tribosensor Using Surface Micromachining
S. Deladi, M.J. de Boer, G. Krijnen, D. Rosén, and M.C. Elwenspoek
J. Micromech. Microeng., vol. **13**(4), pp. S17-S22, 2003

III Precise Magnetoresistance and Hall Resistively Measurements in the Diamond Anvil Cell
S.A. Boye, D. Rosén, P. Lazor, and I. Katardjiev
Rev. Sci. Instrum., vol. **75**(11), pp. 5010-5015, 2004

Conference Contributions

I Complex Target Poisoning Effects in Reactive Sputtering
D. Rosén, O. Kappertz, T. Nyberg, I. Katardjiev, and S. Berg
Presented at the AVS 51st National Symposium in Anaheim, USA, 2004

II Modelling of Sputter Erosion Rate Enhancement from Ceramic Targets
T. Nyberg, O. Kappertz, D. Rosén, T. Kubart, D. Severin, A. Pflug, and S. Berg
Presented at 48th Annual Society of Vacuum Coaters Technical Conference in Denver, USA, 2005

III Influence of Rotating Magnets on Hysteresis in Reactive Sputtering
O. Kappertz, T. Nyberg, D. Rosén and S. Berg
Presented at 47th Annual Society of Vacuum Coaters Technical Conference and 47th Annual Technical Conference in Dallas, USA, 2004

IV A Simplified Treatment of Target Implantation Effects in Reactive Sputtering
O. Kappertz, T. Nyberg, D. Rosén, I. Katardjiev and S. Berg
Presented at the International Conference on Metallurgical Coatings and Thin Films in San Diego, USA, 2004

V Kinetic behaviour of target poisoning during reactive sputtering
D. Rosén, T. Kubart, O. Kappertz, T. Nyberg and S. Berg
Presented at Reactive Sputter Deposition 2005 in Delft, the Netherlands, 2005

VI TRIDYN Simulation of Target Poisoning in Reactive Sputtering
D. Rosén, I. Katardjiev, S. Berg, and W. Möller
Presented at 7th International Conference on Computer Simulation of Radiation Effects in Solids, Helsinki, Finland, 2004

Contents

Introduction

Electro-acoustic devices such as surface acoustic wave (SAW) and bulk acoustic wave (BAW) devices have been in commercial use for over 60 years and can be found in applications ranging from specialised scientific and military equipment to consumer products, such as mobile telephones, TV and radio receivers, etc. Today by far the largest market for electro-acoustic devices is the telecommunication industry which annually consumes approximately three billion acoustic wave filters for frequency control alone.

The development of new materials and technologies for electro-acoustic devices has gained a substantial and growing interest from both academic and industrial research communities in recent years due to the enormous growth in the telecommunication industry and other forms of wireless data communication. One of the bigger issues has been to replace the single crystalline substrates with thin film piezoelectric materials deposited by reactive sputtering. This would not only reduce the manufacturing costs but will also enable high frequency of operation and a wider choice of substrate materials. However, in order to obtain the material properties required for the intended application a detailed theoretical description of the reactive sputtering process is necessary since the texture and other functional properties of the piezoelectric material are extremely sensitive to the process parameters in addition to the structure of the underlying material.

This thesis studies the reactive sputtering process and its application for the fabrication of thin film electro-acoustic devices. The aim has been to gain a further insight into the process and make use of this knowledge to improve the fabrication of electro-acoustic devices. In this work modelling of the reactive sputtering process has been improved by studying certain fundamental aspects of the process and in particular the dynamics of the processes taking place during sputtering both at the target and the substrate surfaces. Consequently, highly textured thin piezoelectric aluminium nitride films have been synthesized and thin film bulk acoustic resonators (FBAR) operating in the GHz range have been fabricated and studied.

Physical Sputtering

Introduction

Sputtering, i.e. removal of surface atoms due to particle bombardment, is caused by atomic collisions at the surface of a target. The process was first reported by W. R. Grove in 1853, who observed metallic deposition within a discharge tube. Thereafter, it took almost 50 years before Goldstein showed that the deposition within the discharge tube was caused by positive ions from the discharge bombarding the cathode. The sputtering process is no longer an unwanted effect destroying cathodes or contaminating plasmas, but is nowadays a widely used method for surface cleaning and deposition of thin films and functional coatings.

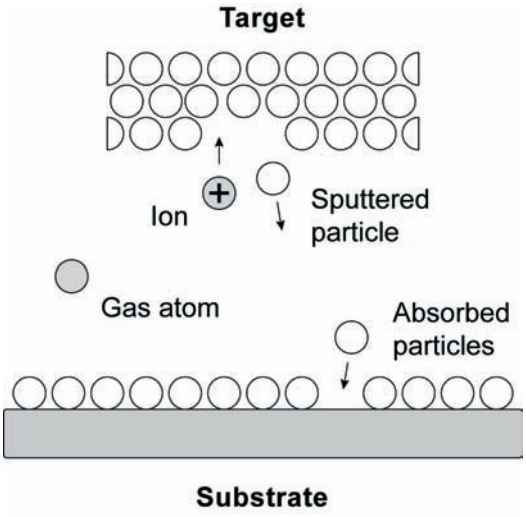

Figure 1. The sputtering process. Positive ions from a gas discharge are accelerated towards a target and create upon impact an atomic collision cascade in which some of the material can leave the target and subsequently condense onto a substrate.

The sputtering deposition process is a physical vapour deposition (PVD) process [1] in which a target material is eroded by a particle bombardment and subsequently deposited onto a substrate, figure 1. In its simplest form a target material is placed in a process chamber filled with a particular process gas at a reduced pressure and set on a negative potential. The negative potential accelerates the few electrons present in the process chamber towards the grounded chamber wall. While traversing the chamber the electrons collide with gas molecules and generate, provided the electric field is sufficiently strong, electron-ion pairs. The ions from the electron-ion pairs are accelerated towards the target and create upon impact with the target surface an atomic collision cascade in which some of the target material can be ejected from the target and subsequently condense onto the surrounding surfaces.

If the electrons solely were generating new charged species in the discharge it would quickly extinguish since the generation of electron-ion pairs would take place closer and closer to the chamber wall and cease when eventually the last electron is collected at the chamber wall. However, while the ions are not able to create electron-ion pairs to the same extent as the electrons, upon impact with the target surface they create secondary emitted electrons which again are accelerated towards the chamber wall and equally so ionize the gas molecules. If the number of secondary emitted electrons per one incident ion times the number of ions created in the discharge is greater or equal to one, the discharge is said to be self-sustained.

A disadvantage of the above described diode sputtering is the relatively low degree of ionization of the process gas. To increase the ionization and thereby the deposition rate a magnetic field is used to confine electrons in the discharge near the surface of the target and hence increase their ionization efficiency. This method, widely known as magnetron sputtering can in addition to increasing the deposition rate also sustain a discharge at a lower pressure compared to non-magnetron sputtering. A low process pressure is usually desirable since the sputtered particles have a long mean free path in a low pressure discharge and can therefore retain some of their kinetic energy as they traverse the process chamber. The excess energy increases the surface diffusion of the absorbed particles at the substrate surface which improves and in many cases promotes crystal growth and the quality of the deposited film [2].

A significant drawback of DC sputtering is that the target must consist of a conducting or a semiconducting material in order to avoid charging [3]. Hence, if an isolating target material is set on a negative potential the ion bombardment quickly charges up the surface of the target eventually resulting in an electrical breakdown in the form of arcing. Arcing can however be avoided by using a radio frequency (RF) or pulsed DC bias. In a RF system the target electrode has a much smaller area than the grounded electrode (chamber walls) and consequently has a much higher current density. The

difference in current densities together with the vastly different ion and electron mobilities result in a large negative self bias of the target surface relative to the plasma and which negative potential acts in much the same way as in DC sputtering to accelerate the ions towards the target surface. In a pulsed DC discharge the target (normally under negative potential) is subjected to a positive pulse for a very short time and hence any excess of a positive charge on the surface is neutralized during this positive pulse.

Reactive Sputtering

Introduction

By adding a small amount of a reactive gas to the sputtering process, such as nitrogen or oxygen, it is possible to deposit compounds from an elemental target material [4, 5]. The reactive sputtering process, however, is a complex process exhibiting a nonlinear behaviour with respect to the main process parameters, such as the partial pressure of the reactive gas, the discharge power etc. In addition, compound is not only formed on the substrate but also on the target surface (target poisoning) and if the target enters the so called compound mode, in which a compound layer is fully formed on the surface of the target, the deposition rate decreases substantially since the sputtering yield for the compound generally is lower then than that of the elemental material. A further characteristic feature of the reactive sputtering process is the presence of hysteresis effects in the process behaviour when operating between the metal mode and the compound mode, as illustrated in figure 2. The hysterisis effects are one of the major problems in high rate reactive sputtering deposition, necessitating a detailed theoretical description of the process and the development of reliable models for optimal process operation.

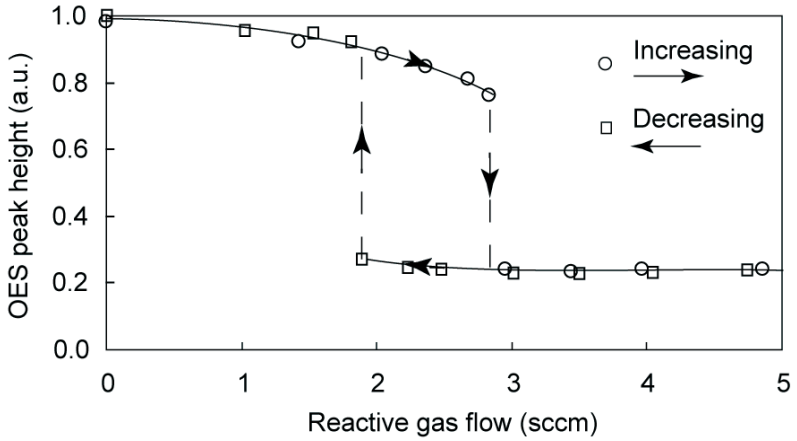

Figure 2. Experimental behaviour of a typical reactive sputtering process. The erosion rate, represented by the optical emission from the sputtered metal atoms, is plotted against the reactive gas flow in standard cubic centimetres per minute (sccm).

Analytical Modelling of Reactive Sputtering

A comprehensive analytical description of the ballistic sputtering process has been developed by P. Sigmund [6]. It describes sputtering of mono-elemental materials as a function of parameters such as mass, energy and angle of the incident ion as well as atomic mass and other properties of the target material. One of the more important results from the model is that for ion energies up to one keV the sputtering yield is approximately given by,

$$\gamma \sim \frac{4 M_1 M_2}{(M_1 + M_2)^2} \times \frac{E}{U_0} \tag{1}$$

where M_1 and M_2 are the masses of the target atom and the incident ion respectively, E the energy of the incident ion and U_0 the surface binding energy of the target material.

Taking into account sputtering alone, however, is insufficient for describing reactive sputtering since its behaviour is strongly dependent on a number of macroscopic system parameters such as gas flow, pumping speed, chamber area, discharge current, etc as well as on a number of microscopic quantities such as sticking coefficients, secondary electron emission, partial sputtering yields, etc. A general model of the reactive sputtering process taking into account all relevant aspects of the process has been developed by S. Berg et al. [7-12]. It describes the reactive sputtering process through a set

of steady state balance equations for both the reactive gas consumption and the mass transport within the process chamber, figure 3 and figure 4. The model, commonly known as the Berg model, has shown an excellent agreement with experimental observations [13, 14] and reached a worldwide acceptance. The flexibility of the model makes it possible to include effects such as reactive sputtering using two targets (co-sputtering) [15] and reactive sputtering in a mixed reactive gas environment [16], etc.

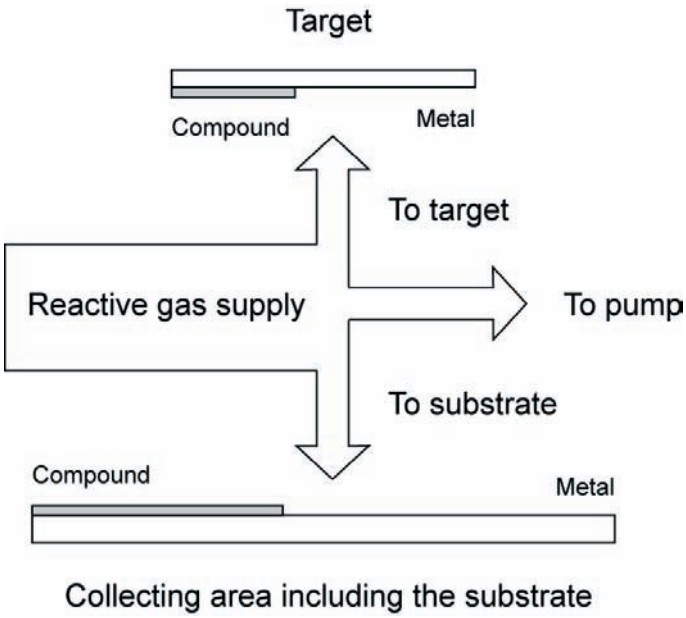

Figure 3. The reactive gas flows in the model developed by S. Berg and co-workers. The reactive gas is either evacuated through the pump or consumed by compound formation on the target or on the substrate.

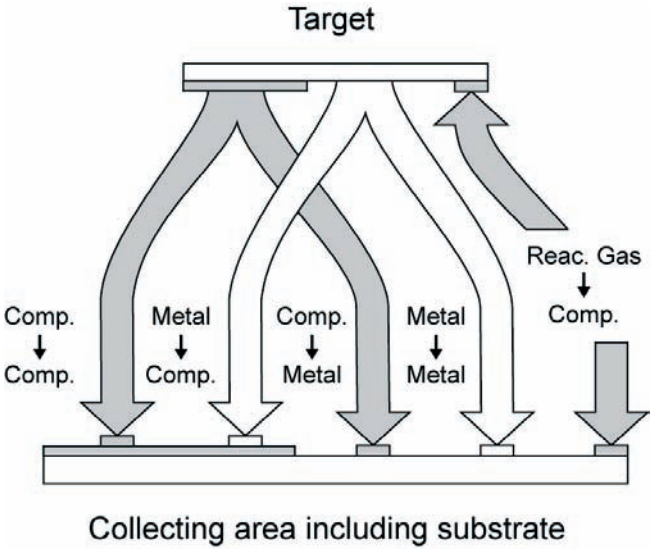

Figure 4. Principle of the mass transport within the process chamber according to the Berg model.

The Berg model is based on a series of assumptions and simplification some of which are straightforward while others require a more thorough explanation. The assumptions made in the model are as follows,

- *The target consists of an elemental metallic material.*

- *Sputtering of the target material is caused by the bombardment of the inert gas ions.*

  Sputtering due to the reactive gas ions is negligible since the partial pressure of the reactive gas normally is much lower than the total process pressure. It has also been shown that the relative sputtering yield of the reactive gas ions is very low [17].

- *The total current, J, is carried by the ions from the discharge and the contribution from secondary electron emission is negligible.*

  This assumption only holds for sputtering of metallic materials since most metals exhibit a relatively low second electron emission coefficient. Compounds on the other hand exhibit a significantly higher coefficient and the calculated sputtering rate will therefore differ from the actual sputtering rate. This can be corrected for by defining an effective sputtering rate for the compound [18, 19].

- *The current is uniformly distributed over the surface of the target.*

  This is not true for magnetron sputtering where the current is mostly concentrated within the race track. The error made by this assumption can, however, be corrected by defining an effective target area, A_t, from which the sputtering takes place [20].

- *The target and the substrate surfaces are divided into two fractions, one which is covered by a compound layer and one being metallic. The compound fraction of the substrate, Θ_s, may differ from the corresponding area on the target, Θ_t.*

- *The metallic fraction of the target and the substrate surface can react with the reactive gas and form the corresponding compound. The reaction probability is defined by the sticking coefficient, α.*

- *The compound formed on the target surface is sputtered as molecules and deposited onto the substrate as such.*

  Studies have given somewhat contradictory results whether compounds are sputtered as molecules or in smaller fractions [21, 22], but the form in which the compound is sputtered has no significant effect on the overall process behaviour.

- *Sputtering of the compound on the target surface exposes the underlying metallic material.*

  In general the compound layer on the target surface is thicker than a few atomic layers, but the thickness of the compound layer can be taken into account by defining sub-layers in the target [23-25].

- *The eroded target material is uniformly distributed onto the substrate, A_s, which includes the total collective area in the process chamber.*

  In most cases the flux of the sputtered particles is only uniformly distributed on a limited area in the process chamber. To realize more realistic results the substrate area must be divided into several sub-areas exhibiting different deposition rates [20].

- *There are no gradients in the partial pressure of the reactive gas.*

Pressure gradients in process chambers have been shown to exist [26], but it is here assumed that the effects from such gradients are negligible when describing the overall process behaviour.

Under these assumptions it is straightforward to derive a set of equations describing the reactive sputtering process. In here we derive the balance equations for the case in which only one target and one reactive gas are considered.

The equations describing the target are given as follows. The reactive gas molecules present in the process chamber react with the metallic fraction of the target surface and form the corresponding compound at a rate,

$$\Gamma\alpha(1-\Theta_t)A_t b \tag{2}$$

where Γ is the flux of reactive gas molecules to the target and b defines the number of compound molecules formed by one reactive gas molecule. Further, the erosion rate of the compound formed on the target surface is given by,

$$\gamma_c \Theta_t A_t \left(\frac{J}{q}\right) \tag{3}$$

where q is the elementary charge and γ_c is the sputtering yield of the compound. At steady state the compound formation rate is equal to the erosion rate of the compound, giving the first steady state balance equation,

$$\Gamma\alpha(1-\Theta_t)A_t b = \gamma_c \Theta_t A_t \left(\frac{J}{q}\right) \tag{4}$$

Equation (4) makes it possible to calculate the fraction of the target covered by a compound layer for any given values of the partial pressure of the reactive gas, provided that the flux of reactive gas molecules is directly proportional to the partial pressure of the reactive gas.

The equations describing the substrate can be derived in a similar manner as that of the target. That is, at steady state the compound formation rate equals the compound "removal" rate on the substrate. The "removal" rate here is not caused by erosion of the compound, as was the case at the target, but is a result of metal deposition into the compound part of the substrate, figure 4. The compound formation rate and the "removal" rate are given by the metal erosion rate, R_c, and the compound erosion rate of the target, R_m, which together give the net erosion rate of the target,

$$R_{target} = R_c + R_m = \gamma_c \Theta_t A_t \left(\frac{J}{q} \right) + \gamma_m (1 - \Theta_t) A_t \left(\frac{J}{q} \right) \quad (5)$$

where γ_m are the sputtering yields of the metal. The compound "removal" rate which corresponds to the amount of metal deposited onto the compound part of the substrate is thereby given by, $R_m\Theta_s$. The decrease of the metallic part of the substrate is in turn given by, $R_c(1\text{-}\Theta_s)$. Note that neither compound deposition onto the compound part of the substrate nor metal deposition onto the metallic part of the substrate affects the overall surface composition of the substrate.

Further, the composition of the substrate is not only altered by deposition onto its surface but can in the same way as the target change due to reaction between the reactive gas molecules and the metallic fraction of the substrate. The rate at which compound is formed by such chemical reactions on the substrate is given by,

$$\Gamma \alpha (1 - \Theta_s) A_s b \quad (6)$$

At steady state the change in the surface composition due to deposition onto the substrate surface balance the compound formation due to the reaction between the metallic part of the substrate and the reactive gas molecules, thus yielding the second balance equation,

$$R_c (1 - \Theta_s) + \Gamma \alpha (1 - \Theta_s) A_s b = \frac{R_m \Theta_s}{d} \quad (7)$$

where d defines the number of metal atoms in a compound molecule.

Although the two balance equations alone describe the average surface composition on the target and on the substrate respectively it is necessary to include the balance equations for the reactive gas flow in order to describe the entire process system. In the model it is assumed that the reactive gas is either evacuated through the pump or consumed by compound formation, as illustrated in figure 3. The number of reactive gas molecules consumed in reactions at the target surface can be written as,

$$Q_t = \Gamma \alpha (1 - \Theta_t) A_t b \quad (8)$$

whereas the corresponding consumption at the substrate is given by,

$$Q_s = \Gamma \alpha (1 - \Theta_s) A_s b \quad (9)$$

Further, the number of molecules evacuated from the process chamber at a partial pressure, P of the reactive gas is given by,

$$Q_p = PS \tag{10}$$

where S is the pumping speed of the pump connected to the chamber. At steady state the contribution from the three different gas consumptions are balanced by the total reactive gas supply, Q, yielding the final balance equation,

$$Q = Q_t + Q_s + Q_p \tag{11}$$

Finally, since the compound fraction of the target and the substrate, Θ_t and Θ_s, can be calculated from the erosion rate of the target and the consumption of reactive gas, it is possible to calculate the total erosion rate R for all given values of the partial pressure of the reactive gas. Typical results from the model are shown in figure 5 and figure 6.

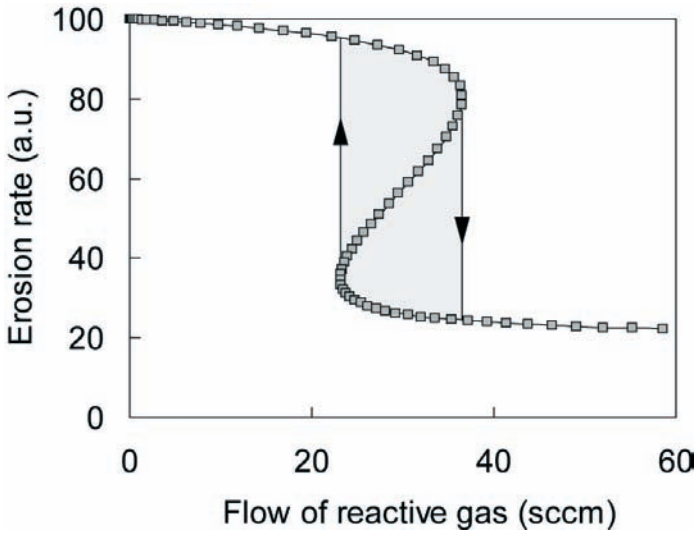

Figure 5. Typical results from the Berg model showing the erosion rate plotted against the reactive gas supply where the hysteresis effect is clearly seen.

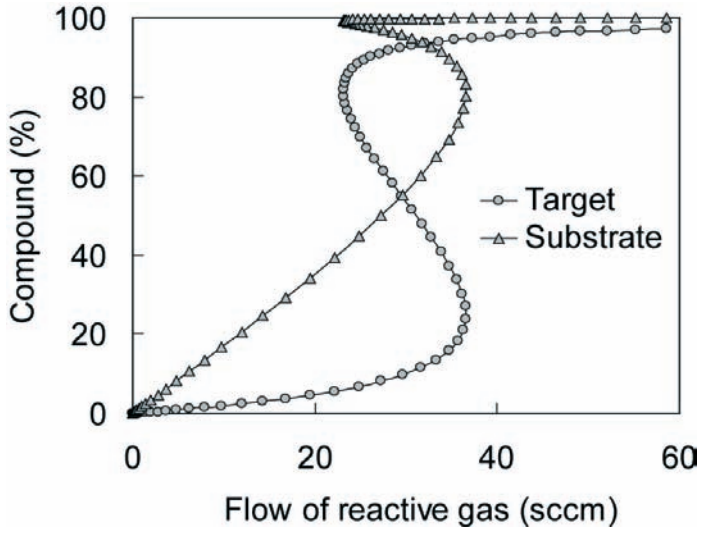

Figure 6. Typical results from the Berg model showing the compound covered fraction of the target and of the substrate plotted against the reactive gas supply.

Numerical Modelling of Reactive Sputtering

The Berg model describes very well, at least quantitatively, the reactive sputtering process at steady state. However, the dynamics of microscopic processes taking place at the target and the substrate surfaces also play an important role. Clearly, the dynamics of such processes is outside the scope of the Berg model and it has to be treated additionally. One very popular and efficient numerical approach in describing the dynamics of the reactive sputtering process is the use of Monte Carlo methods where the macroscopic behaviour of a stochastic process is mimicked by collecting statistics from a large number of randomly selected subprocesses. With respect to sputtering such a subprocess is the atomic collision cascade created as a result of the interaction between an energetic ion and the target material. Further simplifications can be made by approximating the cascade as a sequence of mutually independent binary events, or the so called Binary Collision Approximation (BCA) model [27]. The approximation is used in a number of computer codes, most notably the popular TRIM (Transport of Ions in Matter) program [28]. The TRIM program has shown to give fairly accurate results under normal sputtering conditions and provides a lot of useful information about the sputtering process, such as the ion range profile and the sputtering yield, etc. The static TRIM program, however, cannot describe correctly the dynamics of sputtering and reactive sputtering in particular,

since the concentration depth profile of the target is assumed unaltered by the ion bombardment and which is not the case in reality. Here the dynamic TRIDYN program [29-31] provides a more correct description of the process. The TRIDYN program is based on the static TRIM code and takes into account the particle transport taking place during sputtering by recording and updating the target composition after incoming event. Practically this is done by dividing the target into a finite number of discrete layers which is dynamically updated after each dose increment, see figure 7.

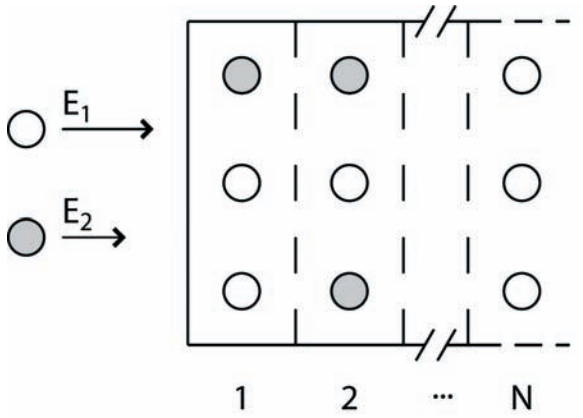

Figure 7. Target discretisation in the TRIDYN program. The target is divided into thin layers which composition is dynamically updated with ion dose.

In order to setup a simulation in the TRIDYN program there is a large number of parameters that have to be defined, such as various specific energies and material constants describing the target and the impinging ions, etc. One of the more important parameters in the simulation is the surface binding energy (SBE) since it to a large extent controls the sputtering yields of the target species, see equation 1. When considering reactive sputtering it is crucial to dynamically define the SBE since the composition of the target evolves continually with dose. It is, therefore, a common practice to define the SBE for the different elements in the target by a matrix model which takes the surface composition and the binding energies between the different elements into account [32],

$$SBE(metal) = C_{reactant} \times SBV_{reactant-metal} + C_{metal} \times SBV_{metal-metal} \quad (12)$$

$$SBE(reactant) = C_{metal} \times SBV_{reactant-metal} + C_{reactant} \times SBV_{reactant-reactant} \quad (13)$$

where $C_{reactant}$ and C_{metal} are the relative surface concentrations of the reactant and the metal respectively and the matrix elements SBV are the binary binding energies between the different elements in the target. One significant drawback of this approach is that the stoichiometry of the compound is not taken into account as it has been shown that the SBE of the different phases in the target exhibit discrete and different values in the transition between the metal mode and the compound mode [33]. The stoichiometry of the compound, however, can be taken into account by redefining the matrix elements SBV but in order to take the discrete behaviour of the SBE into account the SBE must be redefined according to the following equations,

$$SBE(\text{metal in metal mode}) = SBV_{metal-metal} \tag{14}$$

$$SBE(\text{metal and reactant in compound mode}) = SBV_{reactant-metal} \tag{15}$$

$$SBE(\text{reactant in nonreacted mode}) = SBV_{reactant-reactant} \tag{16}$$

In this context it is important to point out that in reactive sputtering, in contrast to nonreactive sputtering, it is not straightforward to derive how different parameters, for example the surface binding energy and the bulk binding energy, relate to each other and the process dynamics. In reactive sputtering there is also often more than one ion species, one of which can react with the target material and thereby change the composition and consequently the sputtering rate of the target. In addition, the impinging ions contribute differently to the erosion rate due to the difference in mass between the different ion species. The contribution from argon bombardment is for example substantially higher than that of nitrogen [17]. Further, the concentration of the reactant is limited by the stoichiometry of the compound. In other words, when full compound mode is reached excess reactive atoms quickly diffuse to the surface or to grain boundaries and are subsequently reemitted. This means that before full compound mode is reached the reactive atoms are removed by sputtering alone, whereas after full compound mode is reached the reactive atoms are removed both by direct sputtering as well as by reemission from the surface. All these effects are to some extent interconnected which makes it hard to formulate a comprehensive description of the reactive sputtering process.

Microstructure and Crystal Growth

The development of reliable models for reactive sputtering is important for many industrial applications. For these applications it is equally important to understand how the microstructure of the deposited film relates to the process conditions. Extensive studies of the correlation between the microstructure evolution and the deposition parameters have been carried out over the past five decades. This has lead to the development of structure zone models (SZM) which relate the microstructure evolution during PVD processes as a function of the growth parameters [34-36]. The structure zone models were originally developed for elemental polycrystalline film growth but can be applied to multielemental film growth as well.

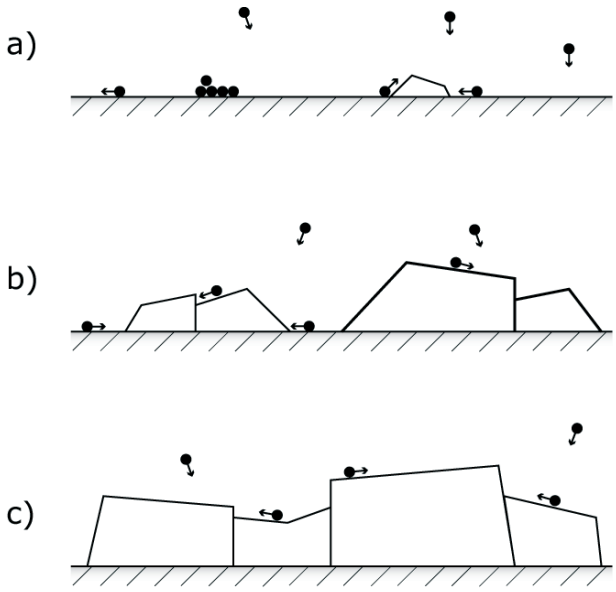

Figure 8. Fundamental processes controlling the microstructure evolution, i.e. nucleation (a) and growth of isolated islands, impingement and coalescence of the islands, formation of polycrystalline islands (b) and the development of continues film structure (c).

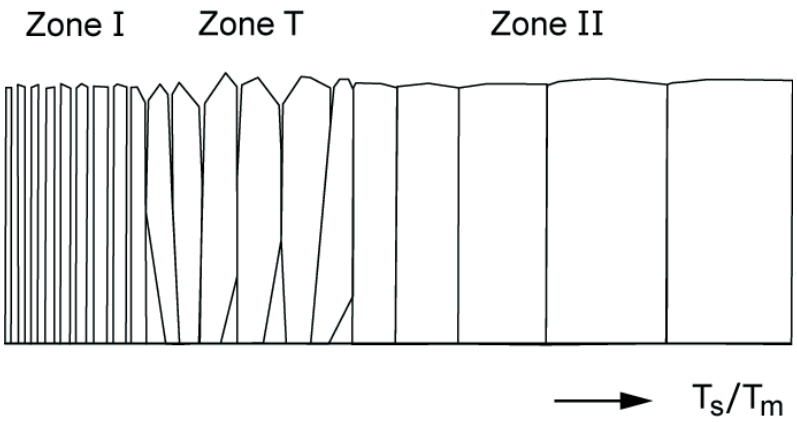

Figure 9. Basic structure zone model, where T_s is the substrate temperature and T_m is the melting point of the deposited film material.

Figure 8 shows the most significant processes controlling crystal growth and the microstructure evolution. The microstructure evolution is to a large extent controlled by the ratio T_s / T_m, where T_s is the substrate temperature and T_m is the melting point of the deposited material, figure 9. In the lower temperature region, Zone I, neither bulk nor surface diffusion has any significant impact on the crystal growth and the film is composed of fibres with a diameter determined by the nucleation density. In the intermediate temperature range, Zone T, the surface diffusion is substantially larger than in Zone I and the faster growing planes dominate the crystal growth though competitive growth. The film is in Zone T characterized by V-shaped grains which develop into a columnar crystal structure as the film thickness increases. The size of the isolated islands in Zone T is considerably larger than in Zone I since the islands coalesce into larger single crystalline islands as the system attempts to minimize the surface and interface energy. In the higher temperature range Zone II, both bulk and surface diffusion are significant and the deposited film exhibits large grain size with a strong degree of texture.

It is important to point out that the orientation of the nuclei on amorphous substrates is almost always random and although single or polycrystalline substrates can promote growth of certain crystal structures the microstructure of the deposited film will eventually evolve towards a state controlled by the process conditions. In addition, in plasma assisted growth processes surface diffusion can be additionally stimulated by the ion bombardment from the plasma, which is one of the greatest advantages of plasma assisted growth, since this allows the deposition of high quality films at reduced substrate temperatures. For example, by lowering the process pressure [2] and/or applying a low energy ion bombardment [36, 37] it is possible to achieve

highly textured films at moderate substrate temperatures. This makes it possible to deposit textured films on substrate that can not sustain high temperatures in addition to solving stress related problems.

Electro Acoustic Devices

Introduction

Electro-acoustic devices such as surface acoustic wave (SAW) and bulk acoustic wave (BAW) devices have been in commercial use for over 60 years. They can be found in applications ranging from specialised scientific and military equipment to consumer products, such as mobile telephones, TV and radio receivers, etc. By far the largest market for electro-acoustic devices is the telecommunication industry which annually consumes approximately three billion acoustic wave filters for frequency control alone. However, one major issue is beginning to set limitations to the current technology. The enormous growth in personal communications systems (PCS) and other forms of wireless data communication have pushed the frequency of operation into the microwave region and made the frequency spectrum increasingly more crowded. This has made the manufacturing techniques for standard devices reaching their practical limits. By way of example, a quartz BAW resonator operating at a frequency of 0.1 GHz requires a device thickness of around 16 microns. To increase the frequency of operation to 1 GHz requires the device to be thinned down to 1.6 microns which only is achievable at very high manufacturing costs. In the case of SAW devices the relatively low acoustic velocity in the currently used materials sets limits on the frequency of operation since the frequency is determined by the acoustic velocity and the lithographic resolution. The development of new materials and technologies for electro-acoustic devices has therefore gained a substantial and growing interest from both academic and industrial research institutes. One of the bigger issues has been to replace the single crystalline substrates with thin film piezoelectric materials. This would not only reduce the manufacturing costs but would also enable better frequency control and a wider choice of substrate materials. The thin film bulk acoustic wave resonator (FBAR) technology is in this respect considered to be the most promising technology, since it can achieve high Q-value resonators, excellent power handling and the possibility for on-chip integration. A comparison of conventional techniques, i.e. ceramic and SAW technology, and BAW technology is given in table 1.

Table 1. Comparison of ceramic, SAW and BAW technologies

	Ceramic	**SAW**	**BAW**
Size	Large	Small	Small
Selectivity	Bad	Very good	Good
Power handling	Very good	Fair	Good
Integration	No	Multi-Chip modules	System-on-Chip
Manufacturability	Mature	Mature	In progress

It should be noted that work on the FBAR technology has been going for more than 30 years, but it was not until the end of last century that the technology attracted a lot of attention for the fabrication of band pass filters for mobile communications in the microwave region. Agilent Technologies, USA, was the first company to start production of such components in 2001. Currently, there are a number of companies [38-41] producing commercially FBAR components for telecom applications.

Film Bulk Acoustic Wave Resonators

FBAR devices are electromechanical resonators which utilize electro-acoustic rather than electromagnetic (EM) resonance. This makes FBAR resonators considerably smaller than EM based resonators since the acoustic velocity is approximately four orders of magnitude lower than the velocity of light. A simple FBAR device consists of a piezoelectric material sandwiched between two electrodes, figure 10. When an alternating electric field is applied between the electrodes, electro-acoustic waves are excited in the piezoelectric material. The fundamental resonance frequency f_r of the thickness mode occurs when $\lambda/2$ is equal to the geometric thickness of the device, where $\lambda=V_t/f_r$ and V_t is the acoustic velocity. The film thickness of a typical FBAR device is in the order of 1 to 2 μm whereas its lateral dimensions are of the order of a few hundred μm. This requires that the resonator is mounted on a carrier substrate for mechanical support which in turn necessitates acoustic isolation of the resonator from the carrier substrate. Depending on the way this acoustic isolation is achieved the FBAR devices are classified as membrane and as SMR (Solidly Mounted Resonators).

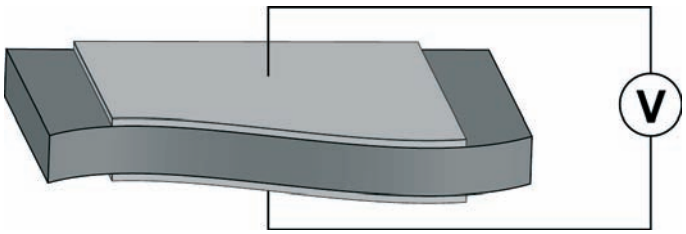

Figure 10. Schematic of a FBAR device. Electro-acoustic waves are excited in the piezoelectric material when an alternating electric field is applied between the electrodes.

Inspecting the S_{11} reflection curve of a typical FBAR, shown in figure 11, one sees that below the series resonance and above the parallel resonance the device behaves as a capacitor while between the two frequencies the device behaves as an inductor. As a result, the impedance phase shifts from -90 degrees to 90 degrees and back again when sweeping the interval between these two frequencies. Both the series and the parallel resonance occurs at 0 degree impedance phase.

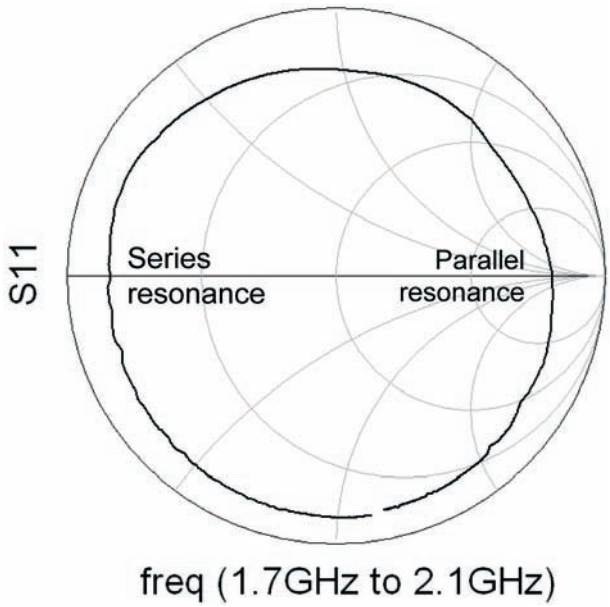

Figure 11. Smith diagram showing measured the S_{11} reflection curve of a typical FBAR resonator.

Membrane FBAR Devices

In this type of devices the resonator is acoustically isolated from the carrier substrate by a cavity (gap). The cavity is formed by bulk micromachining where the substrate underneath the resonator is removed, or alternatively defined by surface micromachining using a sacrificial layer which is removed at the end of the fabrication process. The large difference in acoustic impedance between the electrode material and the surrounding media makes it possible to achieve high Q-values, but the downside is that residual stresses in the film can produce performance deterioration, failure through cracking, etc. In addition, the device can exhibit spurious effects that interfere with the frequency response of the device [42, 43].

Spurious Effects in FBAR Devices

Spurious effects are often observed in FBAR devices having electrode geometries with parallel edges. The effects arise from lateral excited waves that are reflected at the electrode edges and hence give rise to lateral resonant modes. The higher harmonics of these modes can interfere with the operation of the device by generating spurious effects within the operational frequency. The frequencies of the modes are roughly given by,

$$\sim N\frac{v_l}{2h} \tag{17}$$

where N is the mode number, v_l is the velocity of the lateral mode and h is the distance between the two opposite electrode edges. The fundamental resonance frequency of thickness mode is in turn given by,

$$\sim \frac{v_l}{2d} \tag{18}$$

where v_t is the velocity of the longitudinal mode and d is the device thickness. Since the lateral dimension h is much larger than the thickness of the resonator, the higher harmonics of a lateral excited mode can appear close to or within the frequency band of the fundamental longitudinal mode. The lateral exited modes can be suppressed in a variety of ways, most notably by using an asymmetrical electrode geometry where the condition for resonance is not satisfied [43] or by a technique developed by Infineon Technologies together with Nokia in which the lateral modes are suppressed by destructive interference [44, 45]. Figure 12 shows the S_{11} response curve of a resonator suffering from spurious effects.

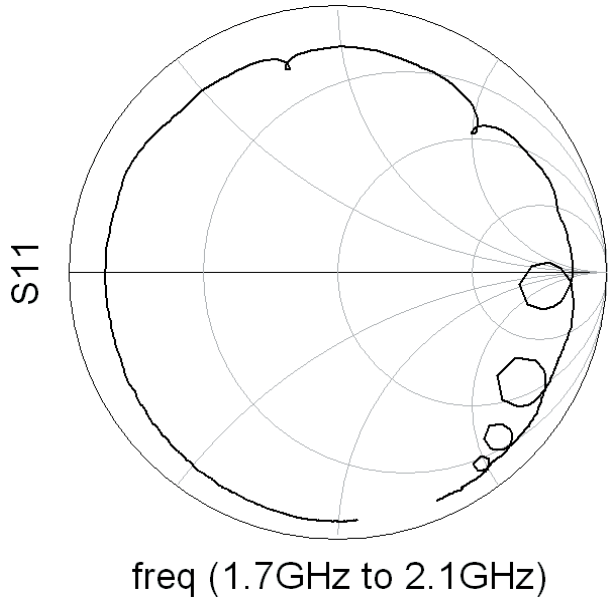

Figure 12. Smith diagram showing the S_{11} response curve of a FBAR resonator exhibiting spurious effects.

Solidly Mounted FBAR Devices

In solidly mounted resonators (SMR) the acoustic isolation to the substrate is achieved by a stack of high and low acoustic impedance layers [41], shown in figure 13 and figure 14. The principle comes from optics where an incident wave is partially reflected at each interface in such a way that all the reflected waves interfere constructively thus defining a mirror. The reflectivity of a so called Bragg reflector where the layers thicknesses are equal to $\lambda/4$ is given by,

$$r = 1 - z^{2N} \tag{19}$$

where z is the impedance ratio between the layers in the reflector and N is the number of stacked pairs. As seen from equation 19 the reflectivity increases with the number of pairs in the stack although in practice it is often sufficient to use three to four pairs.

An advantage of the SMR technology is that the devices are mechanically rigid and not as sensitive to residual stresses in the films.

Figure 13. Principle of the SMR technology. The acoustic waves are reflected by the layer interfaces and summed up by constructive interference.

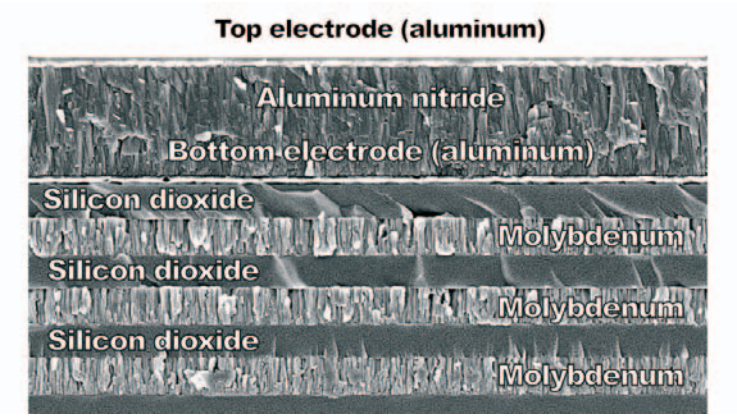

Figure 14. Scanning electron microscope (SEM) cross-section of a working SMR.

Materials for FBAR Devices

When choosing the piezoelectric material for FBAR manufacturing there is a number of factors to be considered. For instance, the material should be compatible with current IC-technology, have a sufficiently high piezoelectric coupling coefficient, k_t, as well as exhibit low intrinsic losses. The material should if possible also exhibit a low temperature coefficient of frequency to minimize the temperature drift. The most commonly used piezoelectric materials in the FBAR technology today are aluminium nitride (AlN), zinc oxide (ZnO) and lead-zirconium-titanate (PZT) the most relevant materials properties of which are presented in table 2. As seen in the table there exists

no ideal material but since neither zinc oxide nor PZT are IC-compatible aluminium nitride has been the obvious choice for telecom applications. Although zinc oxide and PZT have been excluded in our case they have found their way into other areas such as ultrasonic imaging where PZT is extensively used.

Table 2. Comparison of piezoelectric materials used in BAW technology.

	Aluminium nitride	Zinc oxide	PZT
Coupling coefficient k_t^2 [%]	6.5 (bulk) ~6.0 (film)	8.5 (bulk) ~7.5 (film)	8-15
Dielectric constant ε_r	9.5	9.2	80-400
Longitudinal sound velocity [m/s]	11300	6100	4000-6000
Intrinsic material losses	Very low	Low	High
CMOS compatible	Yes	No	No
Temp. coefficient [ppm /°C]	-25	-60	N/A

FBAR Filters

FBAR filters consist of electrically coupled resonators, i.e. ladder filters and lattice filters, or acoustically coupled resonators, i.e. stacked crystal filters. Lattice filters and stacked crystal filters will not be covered in here but a description of these filters can be found in [46] and [47] respectively.

A typical ladder filter consists of two groups of resonators; series resonators and shunt resonators. The term 'series resonator' has in this case no relation to the series resonance frequency, f_s, but indicates instead the position of the resonators in the circuit diagram, figure 15. The resonance frequencies of the two groups are chosen in such a way that the series resonance of the shunt resonators (impedance minimum) matches the parallel resonance of the series resonators (impedance maximum), figure 16. The signal at the edges of the pass band is thereby either reflected or transmitted to ground. The frequency separation between the series and the shunt resonators in the fabrication process is in practice realized by adding a small mass load on top of the shunt resonators which slightly lowers the shunt resonance and anti-resonance frequency. The shunt resonators are detuned by a frequency f_{detune}, which typically is around 80% of the coupling coefficient k_t times the resonance frequency. Outside the pass band the resonators act simply as ordinary capacitors.

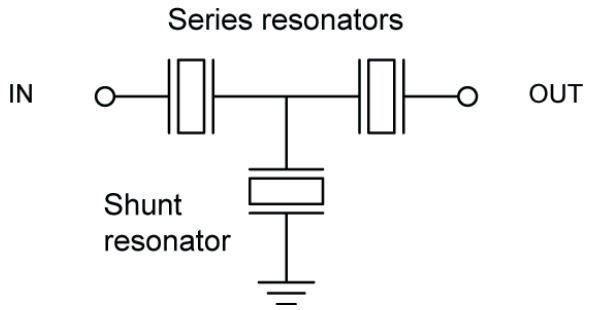

Figure 15. Equivalent circuit of a one T-section ladder filter.

The out of band rejection of a ladder filter is to a large extent controlled by the ratio between the static capacitance of the series and the shunt resonators. It can therefore be improved by increasing the area of the shunt electrodes. Too large ratios can however create problems in the impedance matching of the device. The out of band rejection can also be improved by increasing the number of sections in the filter. This, however, also increases the insertion loss when the internal losses for each stage are added. Further, by choosing the correct number of series and shunt resonators it is possible to avoid contacting the bottom electrode which greatly simplifies the manufacturing process, figure 17.

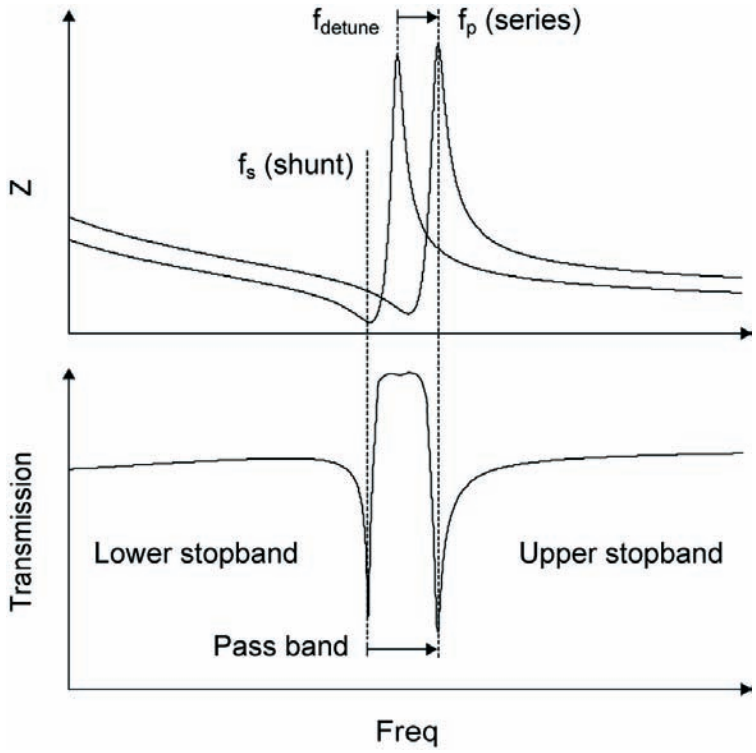

Figure 16. Principle of a ladder filter. The upper graph shows the impedance response curve of the series and the shunt resonators and the lower shows the corresponding filter transmission.

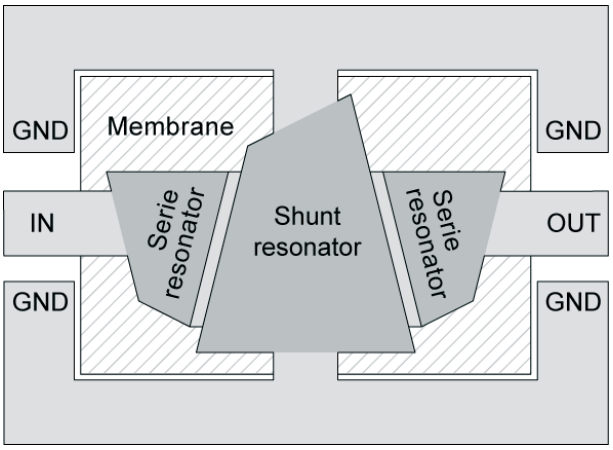

Figure 17. Topology of a 1½ stage ladder filter. The darker areas represent the series and the shunt resonators. The electrode topology is designed to suppress the spurious modes.

Modelling of BAW Devices

The complexity of acoustic waves generated in finite piezoelectric materials has lead to the development of several methods for device modelling. For example, to model the fundamental physical behaviour it is in general necessary to use three-dimensional finite element method (FEM) modelling since it is in practice impossible to analytically describe the fundamental device behaviour [48, 49]. Unfortunately, FEM modelling has shown to be very cumbersome and has had little practical significance in the development of FBAR devices. To describe the general behaviour of the device it is often sufficient to use the one-dimensional electro-acoustic equations, such as the Nowotny and Benes model [50, 51]. A well behaved resonator can also be described by electrical equivalent circuit models, such as the Mason model [52] or the Butterworth van Dyke model [53] which is described below in some detail.

Butterworth van Dyke Model

The Butterworth van Dyke (BVD) model was originally developed for quarts resonators. It is based on an electrical equivalent circuit which consists of a motional arm and a static arm, figure 18. The static arm is given by the clamped capacitance C_0, and represents the capacitor defined by the parallel plate capacitance of the resonator. The motional arm is given by the motional resistance R_m, the inductance L_m and the capacitance C_m, and represents the piezoelectric and acoustic part of the resonator. Note that the elements in the equivalent circuit are interconnected and the only parameter controlled by the designer is the area of the resonator.

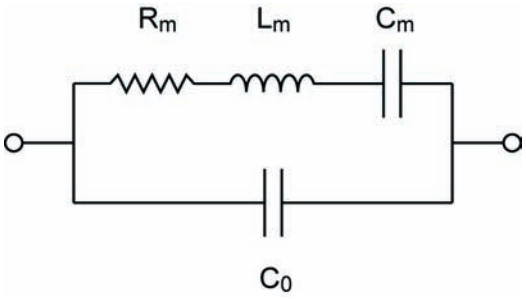

Figure 18. The basic electrical equivalent circuit of a resonator.

In most cases it is necessary to extend the BVD model to include additional parasitic elements since in real life it is not possible of measure the fre-

quency response of an isolated resonator. Figure 19 shows the equivalent circuit of a 1-port resonator including the parasitic losses. In the equivalent circuit the series resistance R_s, represents the contact and resistive losses in the electrodes, R_0 the dielectric losses in the dielectric material and L_s the inductive contribution from the micro strip line. The substrate coupling is described by C_{sub}, R_g and C_g. Note that the equivalent circuit in figure 19 represents a non-symmetrical 1-port device and it is therefore not possible to identify where in the structure the losses occur only that they occur. Nevertheless, the above model is very useful and widely used to characterize electro-acoustic resonators, since the most important parameters such as electromechanical coupling, Q-value, series and parallel resonance frequencies, etc are readily identified in addition to evaluating parasitic losses.

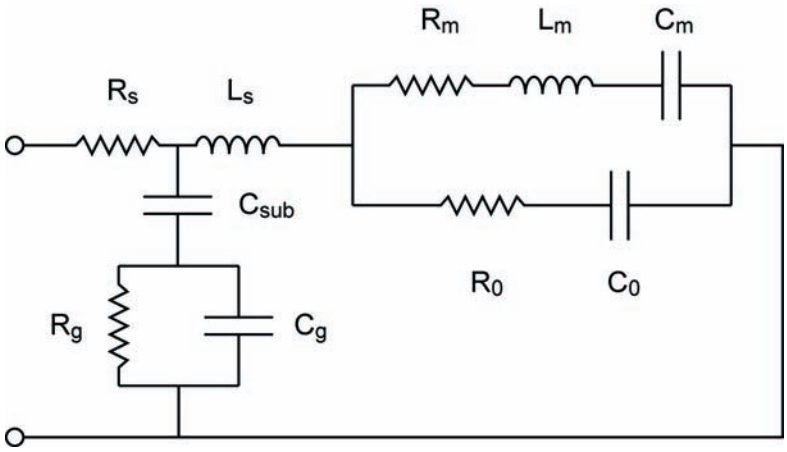

Figure 19. Equivalent circuit of a one port resonator including parasitic effects.

Future of the FBAR Technology

At the end of the nineties it became clear that the standard electro-acoustic technology had reached its practical limits with respect to frequency of operation and that in view of the upcoming generations of mobile communications a new technology was needed for the mass fabrication of electro-acoustic devices in the microwave region. Consequently, at the beginning of the millennium almost simultaneously both in the USA and in Europe the thin film electro-acoustic technology based on the use of piezoelectric thin AlN films was developed. Currently hundreds of millions FBAR filters are fabricated for use in mobile phones and the AlN technology is implemented by the major manufacturers in telecom sector. The above picture creates the

impression that this is the end of story. In fact, nothing can be further from the truth. The fact of the matter is that the current thin film electro-acoustic technology utilizes only one specific acoustic mode, namely the thickness excited longitudinal mode. Taking a look back at the standard electro-acoustic technology, which enjoys a wealth of applications and utilizes a large variety of acoustic modes, each with its own advantages, it is clear that the thin film electro-acoustic technology is yet to realize its full potential. Research in this respect is currently under way and Uppsala University is one of the leading research centers in the field. Already a number of other interesting acoustic modes have been realized using the thin film electro-acoustic technology. Thus, thin film SAW resonators [54] in AlN onto polycrystalline diamond have demonstrated the highest SAW velocity achieved (up to 15000 m/s) thus opening the way for high frequency acoustic devices. The development of tilted AlN films [55] [56] represents a major breakthrough in the field since such films allow the excitation of the thickness excited shear mode and which mode is suitable for operation in liquid media. This in turn opens the way for the development of biochemical sensors. Recently, Lamb waves have been demonstrated [57] in thin AlN membranes exhibiting acoustic velocities of over 10000 m/s in addition to a sufficiently high electromechanical coupling. This makes them very promising for gas sensors.

Thus, it is evident that research in this field is only beginning and a wide range of exciting applications are expected to be developed in the near future.

Summary of Papers

Paper I

In reactive sputtering deposition, target ‘‘poisoning’’, i.e. the formation of compound at the target surface, may reduce the sputter erosion rate substantially and thereby represents a major limitation to achieve high deposition rates. It is known that during reactive sputtering the reactive gas contributes to the formation of compound by both implantation of reactive gas ions into the subsurface layer as well as by chemisorption of reactive gas molecules on the surface of the target. Thus, both chemisorption and ion implantation of energetic reactive ions are the two main mechanisms for the formation of the poisoned layer. In this paper we study theoretically the relative importance of reactive ion implantation and chemisorption in combination with ion induced mixing to the reactive sputtering process.

In order to investigate the formation of the poisoned layer, the TRIDYN program has been employed to simulate the physico-chemical processes that take place at the target surface during sputtering at ion energies which are typical for a magnetron discharge, in a typical gas mixture of Ar with a small (<10%) addition of a reactive gas (e.g. oxygen). The TRIDYN simulations have been performed at varying reactive ion to total ion flux ratio, and at varying ion to reactive neutral flux ratio, for fluences which are sufficiently large to achieve a stationary deposition/erosion balance. The results illustrate that the two mechanisms generate almost identical concentration depth profiles of the poisoned layer, figure 20. They also demonstrate the significance of recoil implantation from the chemisorbed layer for the formation of the compound layer. In agreement with experimental findings, the calculated sputter erosion rate of the target is predicted to decrease monotonically as the partial pressure of the reactive gas increases, see figure 21. The shape of the sputter erosion curve hardly changes between conditions dominated by ion implantation or chemisorption. We therefore conclude that ion implantation basically acts as an additional source of reactive atoms to the target surface. In other words, it does not matter how oxygen is delivered to the target (as an energetic ion or as a chemically absorbed molecule), the effect to target poisoning is effectively the same. Their absolute contributions, however, may be very different depending on the specific process conditions.

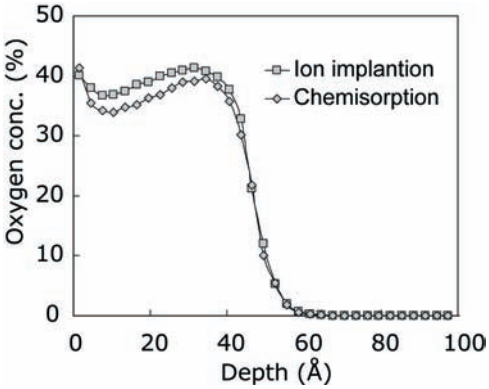

Figure 20. Depth profiles of the oxygen concentration in the target at a partial pressure of oxygen of 3 % and an ion energy of 360 eV.

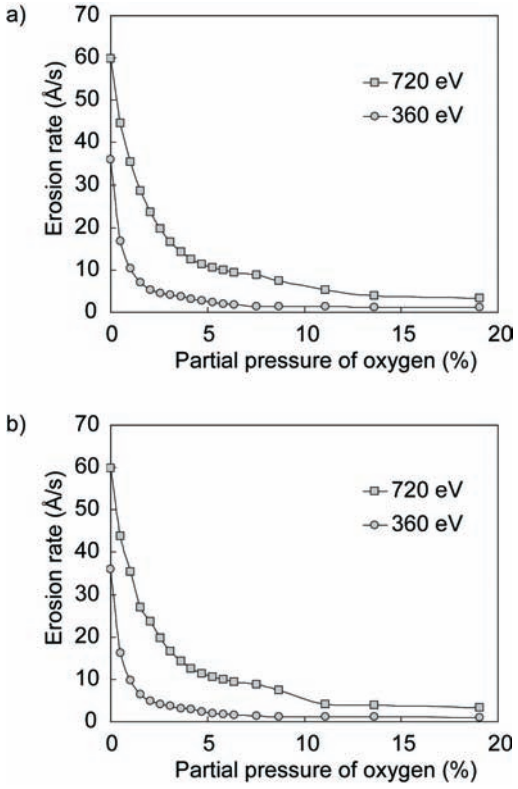

Figure 21. Steady state erosion rates of aluminium plotted against the partial pressure of oxygen. In (a) the oxygen in the simulation ion implanted into the target while in (b) the oxygen is chemisorbed onto the surface.

Paper II

Thin film bulk acoustic wave resonators (FBAR) utilize thickness-excited modes in which the resonance frequency is determined by the thickness of the structure and the wave velocity of the mode used. Unfortunately, other resonant modes may also be excited in the device. Some of these correspond to low-frequency, laterally excited modes and, although a relatively small amount of the total energy is absorbed by these modes, their harmonics may produce an undesirable response around the fundamental resonance frequency of the desired thickness mode. This work explores various ways of suppressing the spurious effects caused by lateral-excited modes by studying their dependence of the electrode geometry.

Aluminium nitride FBAR devices of membrane type using surface micromachining of silicon have been fabricated with various electrode shapes. The frequency response of the devices, given in figure 22 (a) to (d), clearly shows that in order to suppress the lateral exited modes the number of diametrically opposite points with parallel tangents should be kept to a minimum. It is confirmed that resonators with parallel electrode edges exhibit a substantial spurious response due to lateral-mode excitation as well as that resonators which do not have parallel edges suppress effectively the resonance of such modes. It is demonstrated that resonators with an elliptical electrode shape equally suppress lateral excited modes.

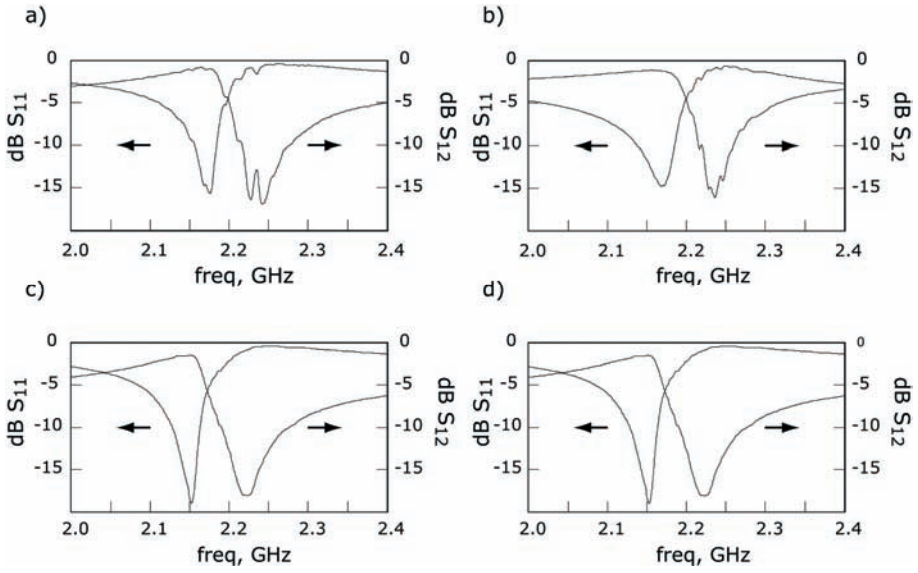

Figure 22. S_{11} and S_{12} response curves from devices consisting of (a) rectangular, (b) circular, (c) irregular and (d) elliptical electrode topology.

Paper III

Thin piezoelectric aluminium nitride (AlN) films are used in bulk acoustic wave (BAW) resonators such film bulk resonators (FBAR) and solidly mounted resonators (SMR). Common requirements for such devices are that they must exhibit low losses and a high electromechanical coupling, properties which are very much dependent of the AlN film quality. The electromechanical coupling, for instance, is directly related to the degree of c-axis orientation of the AlN film for FBAR devices utilizing the thickness excited (TE) longitudinal mode. It is noted, however, that the TE shear mode in thin AlN films is equally interesting particularly for the fabrication of biochemical sensors in which the resonator surface is in contact with a liquid analyte. The goal of this work is to study the variation of the electromechanical coupling and the quality factor of the resonators, for both the longitudinal and the shear modes, as a function of the degree of film texture. The latter is quantified by the FWHM of the rocking curve of the (002) AlN diffraction peak.

Thus, thin piezoelectric AlN films with a predominant c-axis texture have been grown under various conditions by reactive sputter deposition. It was observed that the films exhibit a mean tilt of the c-axis relative to the surface normal, shown in figure 23, and that the mean tilt angle increases both with the distance to the wafer centre and with increasing FWHM of the (0002) rocking curve, figure 24a. FBAR devices have been fabricated to evaluate the electro acoustic properties of the films. The films with a given effective tilt of the c-axis exhibit an electro acoustic behaviour very close to that of a tilted crystal as far as the electro acoustic coupling is concerned. Thus, the electro acoustic coupling of both the shear and the longitudinal mode exhibit the expected couplings for that particular tilt of the c-axis, shown in figure 24b. The shear mode can be excited with a high efficiency in such films opening the possibility for the fabrication of FBAR-based biosensors. The Q factor for the shear mode is observed to decrease with film tilt.

This work laid the grounds for the development of an elegant and a original method for the deposition of AlN thin films with a tilted c-axis [56].

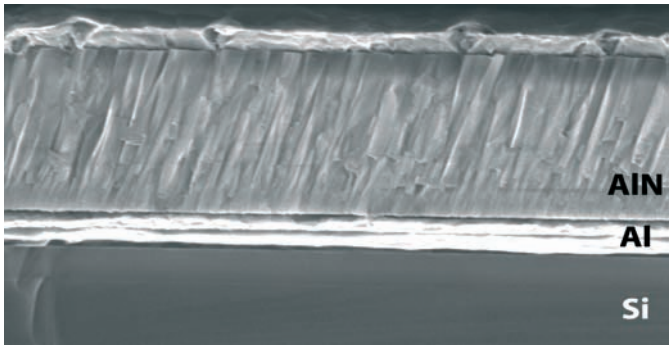

Figure 23. A cross-sectional SEM of a 2-µm thick aluminium nitride film exhibiting tilted columnar growth.

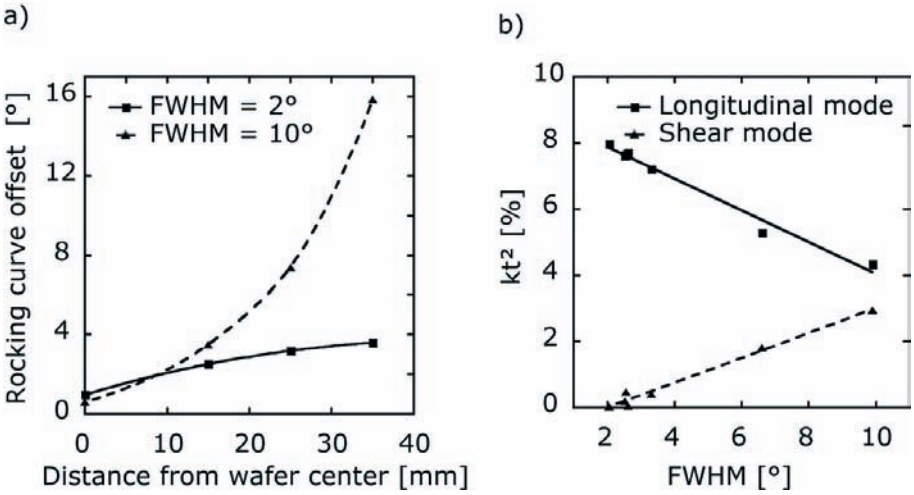

Figure 24. FWHM offset as a function of distance from wafer centre for two films with different textures a), and the electromechanical coupling of the shear and longitudinal modes as a function of the FWHM (002) rocking curve, b).

Paper IV

Reactive sputtering is a process exhibiting a complex behaviour as a function of the process parameters. Studying the dynamic behaviour of the process is commonly done by programs based on numerical methods, such as the Monte Carlo program TRIDYN. In TRIDYN simulations of reactive sputtering it is typically assumed that the surface binding energy (SBE) for the different phases formed on the target surface exhibits a linear behaviour in the transition between the metal mode and the compound mode. In this work we study how the transition between the two modes takes place and more specifically attempt to experimentally identify how the SBE for the different phases behaves in the transition between the two modes. In essence, this is done by comparing XPS measurements of the aluminium 2p binding energy on samples comprising pure aluminium, stoichiometric aluminium nitride and aluminium oxide with the corresponding measurements on under stoichiometric aluminium nitride samples. In this work it is assumed that the binding energy of the core level is directly correlated with the SBE of the phase in question. That is to say, if the aluminium 2p binding energy in aluminium nitride exhibits a constant and discrete value independent of the nitrogen concentration, the SBE for the compound exhibits a constant and discrete value independent of the surface concentration of nitrogen. This is the so called discrete model, i.e. the Al atoms are either in pure compound or in pure elemental states and the corresponding probability is a linear function of the relative concentrations. Alternatively, if the SBEs are functions of the relative concentrations then it is assumed that a homogeneous phase is predominantly formed at the target surface. This assumption forms the basis of the so called analogue model.

It was found by the XPS measurement that the aluminium 2p binding energy in aluminium nitride indeed exhibits a constant and discrete value independent of the nitrogen concentration in the samples and it was therefore concluded that the SBE for the different phases exhibit constant and discrete values independent of the surface concentration of nitrogen, figure 25 and figure 26. The discrete behaviour of the SBE was implemented in the TRIDYN program and the results from these simulations were compared with simulations in which it is assumed that the SBE of the different phases exhibit a linear behaviour in the transition between the metal mode and the compound mode. It was found that if the discrete model is assumed, the erosion rate of the target is a linear function of their relative concentrations. If the analogue model is assumed the erosion rate exhibits a somewhat more complex, generally nonlinear function of their relative concentrations.

The XPS findings together with the simulations indicated that in the case of aluminium nitride the discrete model describes correctly the compound formation at the target surface.

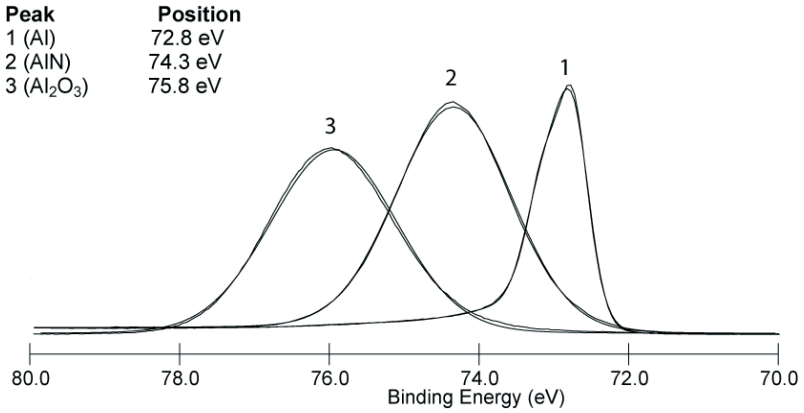

Figure 25. The XPS binding energy spectra of the aluminium *2p* orbital for the pure phases, (1) aluminium, (2) aluminium nitride and (3) aluminium oxide. The splitting of aluminium *2p* orbital can be seen as a bump on the left side of the aluminium peak (1).

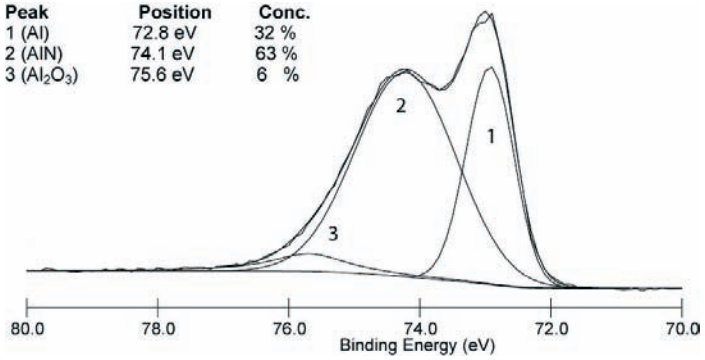

Figure 26. The XPS binding energy spectra of the aluminium *2p* orbital in an under stoichiometric aluminium nitride sample. The sample was deposited at a DC power of 1200 W, at 5 mTorr, and a gas flow of 10 sccm nitrogen and 90 sccm argon.

Paper V

The right choice of surface passivation material for silicon carbide (SiC) high voltage devices is challenging due to the high critical fields the passivation material must sustain. The dielectric should in this case be characterised by a high breakdown field, a high dielectric constant and be able to block electric field penetration into the space above the surface of the working semiconductor device. Today the most commonly used passivation material in microelectronics is silicon dioxide. Its applicability in the silicon technology is well established, but nevertheless its use for the passivation of high power devices in SiC is problematic due to the 2.5 times lower dielectric constant than SiC, 3.9 for silicon dioxide and 10 for SiC. For this reason new insulating materials with higher dielectric constant are being investigated where especially aluminium oxide ($\varepsilon_r \approx 8$) and aluminium nitride ($\varepsilon_r \approx 9.14$) are considered as potential substitutes for silicon dioxide. This work focuses on aluminium nitride (AlN) as a surface passivation material deposited by reactive sputtering.

In this work a 190 nm thick AlN layer was deposited on n and p type (100) silicon and on n type 4H-SiC samples. The metal-insulator-semiconductor (MIS) structures made on the samples were analysed by I-V and C-V techniques and SiC diodes were used to evaluate leakage current before and after the AlN deposition.

Prior to the deposition all samples were exposed to UV light and half of the samples were also exposed to a 5% HF solution. It was concluded that the HF treatment made prior to the deposition did not influence the I-V characteristics of the silicon samples but the non-HF etched p-type silicon sample, however, is characterised by a 2.5 times smaller C-V hysteresis loop compared to the corresponding HF etched samples.

Even though the devices presented in this study did not show optimal performance there are clear indications that if correctly optimized low temperature deposited AlN may serve as a passivation material for SiC power devices. In fact, in the continuation of this work the aluminium nitride process was modified by applying a bias to the substrate during processing. The additional ion bombardment suppresses crystal growth of the aluminium nitride film which subsequently did not show any peeks in the XRD measurement. Devices based on this new process showed excellent performance and could sustain fields in excess of 3 MV/cm, which is the bulk break down field of SiC. This very promising result opens the way for significant improvements in the performance of high voltage SiC devices. These latest results will be published in a forthcoming article.

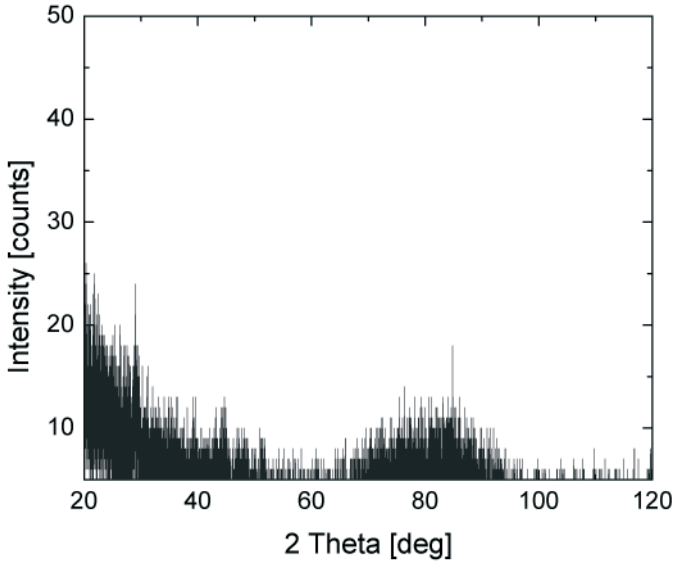

Figure 27. Crystal grows of the deposited aluminium nitride film was prevented by applying a bios to the substrate during processing. The XPS measurement therefore did show any peeks in the θ-2θ spectra.

Paper VI

By adding reactive gas, such as oxygen or nitrogen, to the conventional sputtering process it is possible to perform reactive sputtering. The purpose of the reactive gas is to react with the deposited metal and form the corresponding compound (oxide or nitride etc). Unfortunately, the reactive gas also reacts with the metal at the target surface and since the compound generally has a lower sputtering yield than the metal, this reduces the sputter erosion rate from the target. In addition, it is a well known fact that the relationship between the reactive gas flow and the other processing parameter is very complex and non-linear, and usually exhibits hysteresis effects.

Instead of using a metallic target to obtain a compound film, it is possible to use a ceramic target that already has the desired composition. Usually one has to add a small amount of the reactive gas to ensure that the growing film is fully stoichiometric. However, this approach has both advantages and disadvantages. Among the advantages is the absence of hysteresis effects which makes the process very easy to control. A disadvantage may be the modest deposition rate and it could also be problematic to perform sputtering from non-conducting targets. One might think that the sputter erosion rate from a ceramic target would be almost identical to the erosion rate that is obtained from a metallic target operating in fully stoichiometric mode in reactive sputtering, but there are several reports disclosing a surprisingly high deposition rate of compound films from ceramic targets. The purpose of this work is to obtain a more detailed understanding of the underlying mechanisms during sputtering from a ceramic target.

In this work we present a model for reactive sputtering from ceramic targets. Previously, we assumed that the compound formed at the target surface is sputtered as molecules. In the new model it is assumed that the compound is not sputtered as molecules, but as metal atoms and reactive gas atoms with different sputtering yields. The different sputtering yields for the metal atoms and the reactive gas atoms were estimated by TRIDYN simulations. The model can predict the surprisingly high deposition rates that have been reported by others. In short, the reason for the high rate is that the different sputtering yields give a more metallic target surface as compared to the bulk composition due to preferential sputtering of reactive gas atoms. This means that the target surface has metal atoms that are not chemically bonded to the reactive gas atoms. These “free” metal atoms have higher sputtering yield than the metal bonded to reactive gas atoms. Consequently, the sputter erosion rate, and subsequently the deposition rate, is higher than from a completely compounded surface.

Paper VII

The reactive sputtering process is one of the most commonly used techniques for deposition of oxides, nitrides, carbides, etc. It is, however, a well known fact that the relationship between the reactive gas flow and the other processing parameter is very complex and non-linear and usually exhibits hysteresis effects. The steady state relation between the different parameters has been extensively studied and existing models are capable to describe and predict most processing behaviour.

Recently, it has become very common to use moving magnets behind the target to promote uniform consumption and a high degree of utilization of the target material. In some applications, e.g. the cylindrical magnetron targets used for large area deposition, the magnets are fixed while the target is moved. The principle is the same for both arrangements, only a fraction of the target is sputter-eroded at any given point in time and the sputter erosion zone moves around over the target surface. This means that an arbitrary point at the target surface only will be periodically exposed to ion-bombardment (sputter erosion) for some time. Between two such occasions, the target will be exposed only to reactive gas, and compound will form at the target surface. Thus, each point of the target surface will have a periodic compositional behaviour. It is the purpose of this work to obtain a more detailed understanding of how parameters, like the rotational speed, influence the hysteresis effect and other properties of the reactive sputtering process, when moving magnets are used behind the target.

By combining previously presented models for the static behaviour of the reactive sputtering process with a model describing the time dependent behaviour of the target, it is possible to describe the reactive sputtering process when the sputter eroded area is moving with respect to the target surface. In this work, we have implemented such a model and compared the results of the calculations with experimental data.

It has been shown that the speed of the erosion zone influences the reactive sputtering process so that the hysteresis region is shifted. This behaviour is in agreement with experimental findings. Under certain conditions, this effect may shift the complete process from metal mode to compound mode if the speed is changed during sputtering.

Paper VIII

In this work we present a study of the dynamic behaviour of a metallic target operating in reactive sputtering. This was done since there so far have not been any detailed studies of the dynamic properties of the surface of the target despite that its dynamic behaviour represents a key factor in the development of reliable process control.

In this study we focus on the dynamic behaviour of the near surface region of a titanium target and especially study the difference between chemisorption and ion implantation of the reactive gas, in this case nitrogen, in the process. Two sets of simulations have been carried out in the TRIDYN program, one considering chemisorption at the target surface only and the other considering ion implantation of the reactive gas alone. In both cases the target was simultaneously exposed to bombardment of energetic argon ions.

In the simulations it was found that there were only small differences in the dynamic behaviour before reaching steady state and equally so at steady state between non-energetic nitrogen and the energetic nitrogen case. It was concluded that the energetic argon ion bombardment caused both a knock-in effect of gas atoms adsorbed at the target surface as well as atomic mixing of the reactive gas atoms in the subsurface region. This caused the depth profile of the adsorbed reactive gas atoms to reach the same depth as that for the implanted reactive gas ions. One might think that a difference in the behaviour between the two cases should be a result from the additional sputter erosion caused by the energetic nitrogen ions, but it turns out that the energetic nitrogen stands for less than 5 % of the total erosion of the Ti atoms from the target and it was therefore concluded that the influence of the nitrogen supply on depth thickness and profile was quite insensitive to how the nitrogen was supplied to the target.

Acknowledgements

I have met and got to know many people over the years I have been working at the department of Solid State Electronics. Here I want to acknowledge some of the people that I feel have greatly influenced my work.

Sören Berg, your laidback attitude towards research and work in general has been refreshing and resulted in some really good research.

Ilia Katardjiev, for me you have been the ideal supervisor. You have had strong opinions about what and how things should be done, but have in the end let me have my way (or made me believe that).

Fellow co-workers and friends at the Department, it is you who have made my work at the department worth the effort, for even the most interesting job gets boring if you don't have someone to share it with.

The research engineers, I have always admired your readiness to help.

The people at Twente, the Netherlands, have meant surprisingly much to me, both professionally and privately. It has been one of the highlights during my PhD study.

Uppsala 2006
Daniel Rosén

Sammanfattning på svenska

Denna avhandling består av studier av beläggningsmetoden ”reaktiv sputtring” samt av så kallade elektroakustiska komponenter. Båda dessa delar kommer att få en kort introduktion följt av en sammanfattning av de artiklar som ingår i avhandlingen.

Reaktiv sputtring

Sputtring benämner den eroderingseffekt som sker då ett material utsätts för ett jonbombardemang. Positivt laddade joner som genereras i ett plasma accelereras mot den negativt laddade katoden. Då de träffar katoden skapas en atomär kollisionskaskad där en del av katodmaterialet stöts ut och vidare absorberas på de omkringliggande ytorna, se figur 28.

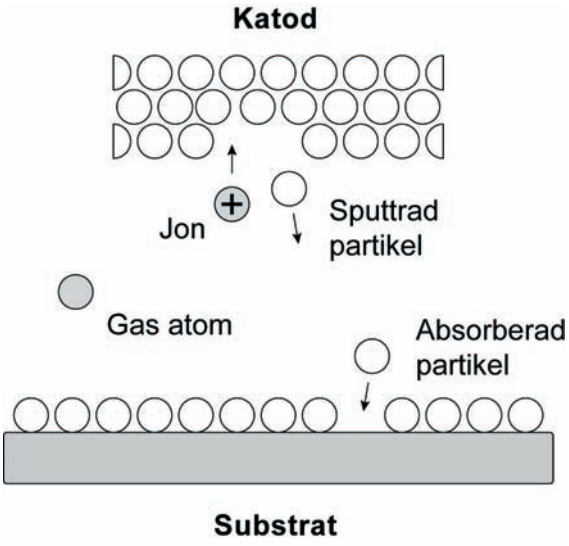

Figur 28. Principen för sputtringseffekten. Joner som genereras i ett plasma accelereras mot en katod och skapar där en atomär kollisionskaskad i vilket en del av katodmaterialet stöts ut och absorberas på substratet.

Genom att tillsätta en reaktiv gas som syre eller kväve till processen är det möjligt att belägga ett keramiskt material från en metallisk katod. Reaktiv sputtring är dock en komplicerad process vilket kräver noggranna studier för att uppnå de önskade egenskaperna hos det deponerade materialet.

Bulkakustiska komponenter

Bulkakustiska komponenter, figur 29, är elektroakustiska komponenter som har blivit allt mer uppmärksammade genom den snabba utvecklingen inom telekomindustrin. Denna uppmärksamhet kommer sig av att de nu använda komponenterna, så som keramiska och ytakustiska komponenter, har börjat nå sin praktiskt tillämpningsbara gräns då arbetsfrekvensen för komponenterna pressats allt högre.

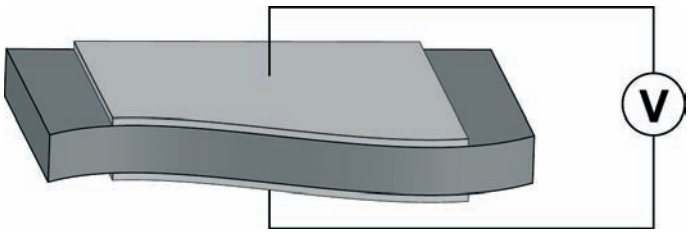

Figur 29. Principen för en enkel bulkakustisk resonator där det piezoelektriskt material är beläget mellan två elektroder.

Det har dock visat sig att övergången till bulkakustiska komponenter inte är helt enkel och kräver noggranna studier av så väl deponeringsteknik som av komponentdesign. Med detta som bakgrund har Tunnfilmsgruppen, tillsammans med Ericsson, studerat elektroakustiska komponenter. Fokus på arbetet har legat på utveckling av tillverkningsprocesser för så kallade tunnfilmsbulkakustiska komponenter samt på komponentdesign.

Papper I

I denna artikel har vi med hjälp av datorsimuleringar undersökt hur keramiska material bildas på ytan av en metallisk katod vid reaktiv sputtring. Detta gjordes för att det tidigare har varit oklart huruvida keramen bildas genom kemisorption av den reaktiva gasen eller genom direkt jonimplantering. Simuleringarna gjordes med hjälp av simuleringsprogrammet TRIDYN där vi valt att studera reaktiv sputtring av aluminiumoxid från en aluminium katod. I simuleringarna har vi varierat förhållandet mellan argon och syre i processgasen och studerat tjockleken och stökiometrin av den keram som bildats på katodytan.

I studien visade det sig att keramen som bildas genom kemisorption var mycket lik den som bildas genom direkt jonimplantering. Detta kan förklaras av att jonbombardemang som härrör från argonjonerna rör om ytlagret på katoden så att det är när på omöjligt att skilja de två effekterna åt. Det visade sig även att den eroderingen som orsakas av syrejonerna är mycket låg.

Papper II

I denna artikel har vi studerat de lateralt exciterade moderna som oönskat kan uppkomma i bulkakustiska komponenter. Dessa moder uppstår ofta i eller omkring arbetsfrekvensen för komponenten och skapar där rippel i frekvensresponskurvan. Eftersom de lateralt exciterade moderna endast uppkommer mellan motstående elektrodkanter kan dessa undertryckas genom att designa topologin på elektroderna med en viss grad av osymmetri. Vi har jämfört olika elektrodsymmetrier och visat att både en elliptisk och en osymmetrisk rektangulär geometri kan användas för att undertrycka de laterala moderna. Kvadratiska och cirkulära elektrodgeometrier visar som väntat rippel i frekvensresponskurvan.

Papper III

I denna artikel har vi studerat texturen av den piezoelektriska aluminiumnitridfilm som används i bulkakustiska komponenter och relaterat denna till de resonanta moder som exciteras i komponenterna. Detta gjordes genom att tillverka och utvärdera komponenter med olika textur på aluminiumnitridfilmen. Vi har även visat att det under vissa förhållanden var möjligt att excitera skjuvmoden, vilken ofta används i biosensorer, även om det van-

ligtvis endast är den longitudinella moden som exciteras i bulkakustiska komponenter.

Papper IV

I denna artikel har vi studerat hur ytbindningsenergin hos keramiska material varierar med stökiometrin. Detta gjordes genom att tillverka aluminiumnitridfilmer med olika stökiometri. Med hjälp av röntgenstrålningsspektroskopi uppmättes sedan bindningsenergin hos aluminium *2p* orbitalet. Detta gjordes för att man tidigare vid simulering av reaktiv sputtring antagit att bindningsenergin hos katod materialet har en linjär övergång från den metalliska moden till den keramiska moden. Det visade sig dock att elementen i keramen antog konstanta värden på bindningsenergin i övergången mellan moderna. Det binära beteendet hos bindningsenergin implementerades i simuleringsprogrammet TRIDYN och resultaten från simuleringarna jämfördes med det linjära fallet.

Papper V

I denna artikel har vi studerat huruvida aluminiumnitrid kan användas för passivering av högspända kiselkarbidkomponenter. Detta gjordes för att kiseloxid, vilket idag är det vanligast förekommande materialet för passivering av högspända kiselkarbidkomponenter har en mycket lägre dielektrisk konstant jämfört med kiselkarbid. Denna skillnad i dielektrisk konstant ställer onödigt höga restriktioner för komponentdesignen.

I detta arbete har en 190 nm tjock aluminiumnitridfilm deponerats på n- och p-typ kisel samt på 4H-SiC prover. MIS komponenter som tillverkats av proverna utvärderades genom att studera I-V och C-V karakteristiken. SiC dioder användes för att utvärdera läckströmmarna genom materialen både före och efter aluminiumnitriddeponeringen.

Före aluminiumnitriddeponeringen behandlades vissa av proverna med en 5 % HF lösning. Det visade sig att HF behandlingen inte påverkade I-V karakteristiken, men hade en viss inverkan på CV karakteristiken. De komponenter som tillverkats av p-typ kisel och inte HF behandlats uppvisade en 2.5 gånger mindre hysteresiseffekt jämfört med de komponenter som HF behandlats. Även om komponenterna i studien inte visade optimal prestanda finns det klara indikationer på att med vidare optimering av processen kan aluminiumnitrid användas för passivering av högspända kiselkarbidkomponenter.

Papper VI

Genom att tillsätta reaktive gas till en konventionell sputtringsprocess är det möjligt att deponera keramiska material från en metallisk katod. Som ett alternativ till att använda en metallisk katod är det möjligt att använda en katod tillverkad av det keramiska material som man önskar belägga. Detta förenklar processningen genom att ta bort det olinjära processbeteendet som reaktiva sputtring normalt uppvisar, men det sänker å andra sidan deponeringshastigheten för processen.

På senare tid har det kommit rapporter som visar på en högre deponeringshastighet än vad som skulle kunna förväntas vid användandet av en keramisk katod. I detta arbete har vi undersökt de underliggande orsakerna till denna oväntat höga deponeringshastighet och presenterar även en modell som beskriver processen.

I tidigare modeller har vi antagit att keramiska material sputtras i form av molekyler, men det har dock visat sig att keramen sputtras i sina atomära beståndsdelar. Genom att implementera detta i tidigare använda modeller har vi kunnat visa hur den oväntat höga deponeringshastigheten uppkommer. Det visade sig att ytlagret på katoden utarmades på reaktiva atomer vilket i sin tur ökade deponeringshastighet.

Papper VII

Reaktiv sputtring är en av de mest använda teknikerna för deponering av keramiska material. På senare tid har det blivit allt vanligare med användandet av cylindriska katoder vilka roterar under processningen. Detta görs för att förbättra uniformiteten på den deponerade filmen samt för att bättre utnyttja katodmaterialet. Detta för dock med sig att delar av katoden periodvis exponeras för enbart den reaktiva gasen och på dessa ytor bildas då en tunn keram. Syftet med detta arbete är att i detalj studera dynamiken hos en roterande katod och presentera en modell som beskriver tidsberoendet hos processen.

Genom att kombinera en modell som beskriver det statiska beteendet med en modell som beskriver det dynamiska beteendet hos reaktiv sputtring är det möjligt att beskriva tidsberoendet hos processen. Resultaten från den kombinerade modellen visar att rotationshastigheten på katoden starkt påverkar hysteresiseffekten. Resultaten är i linje med experimentella resultat.

Papper VIII

I denna artikel har vi studerat det dynamiska beteendet av en metallisk katod under reaktiv sputtring. Detta gjordes för att det tidigare inte har presenterats någon studie av katodens dynamiska beteende även om detta är avgörande för utvecklingen av en stabil process.

I studien har vi genom simuleringsprogrammet TRIDYN undersökt skillnaden mellan kemisorption och jonimplantering av den reaktiva gasen vid reaktiv sputtring. Detta gjordes genom att jämföra simuleringar där enbart kemisorption togs i beaktning med simuleringar där den reaktiva gasen var jonimplanterades i katoden.

Studien visade att det endast var små skillnader i det dynamiska beteendet mellan kemisorption och jonimplantering av den reaktiva gasen och att även jämviktstillstånden i de två fallen uppvisade ett likartat beteende. Som slutsats kunde det dras att den mixning av ytlagret som orsakas av argonjonbombardemanget gjorde att det inte gick att särskilja några skillnader mellan kemisorption och jonimplantering av den reaktiva gasen vid reaktiv sputtering.

References

[1] R. Parsons, "Sputter Deposition Processes," in *Thin Film Processes II*. Eds. CA, USA: Academic Press Limited, 1991.

[2] G. F. Iriarte, F. Engelmark, and I. V. Katardjiev, "Reactive sputter deposition of highly oriented AIN films at room temperature," *Journal of Materials Research*, vol. 17, pp. 1469, 2002.

[3] P. C. Johnson, "The Cathodic Arc Plasma Depostition of Thin Films," in *Thin Film Processing*, vol. 2. San Diego: Academic Press, Inc., 1991.

[4] I. Safi, "Recent aspects concerning DC reactive magnetron sputtering of thin films: a review," *Surf. Coat. Technol.*, vol. 127, pp. 203-18, 2000.

[5] S. Berg, T. Nyberg, H.-O. Blom, and C. Nender, "Modeling of the Reactive Sputtering Process," in *Handbook of Thin Film Process Technology*. Bristol, UK: Institute of Physics Publishing, 1998.

[6] P. Sigmund, "Sputtering by Ion Bombardment: Theoretical Concepts," in *Sputtering by Particle Bombardment*, vol. 47, *Topics in Applied Physics*. Berlin: Springer-Verlag, 1981.

[7] S. Berg, H.-O. Blom, T. Larsson, and C. Nender, "Modeling of reactive sputtering of compound materials," *J. Vac. Sci Technol. A*, vol. 5, pp. 202-207, 1987.

[8] S. Berg, T. Larsson, C. Nender, and H.-O. Blom, "Predicting thin-film stoichiometry in reactive sputtering," *J. Appl. Phys.*, vol. 63, pp. 887-891, 1988.

[9] H. Bartzsch and P. Frach, "Modeling the stability of reactive sputtering processes," *Surf. Coat. Technol.*, vol. 142-144, pp. 192-200, 2001.

[10] V. A. Koss and J. L. Vossen, "A model for simultaneous reactive sputtering, etching, and chemical vapor deposition," *J. Vac Sci Technol. A*, vol. 8, pp. 3791-5, 1990.

[11] H. Ofner, R. Zarwasch, E. Rille, and H. K. Pulker, "A reactive sputtering model applied to AlN," *J. Vac Sci Technol. A*, vol. 9, pp. 2795-6, 1991.

[12] H. Sekiguchi, T. Murakami, A. Kanzawa, T. Imai, and T. Honda, "Computational modeling of reactive gas modulation in radio frequency reactive sputtering," *J. Vac Sci Technol. A*, vol. 14, pp. 2231-4, 1996.

[13] R. Mientus and K. Ellmer, "Reactive DC magnetron sputtering of elemental targets in Ar/N_2 mixtures: Relation between the discharge characteristics and the heat of formation of the corresponding nitrides," *Surface and Coatings Technology*, vol. 116-119, pp. 1093, 1999.

[14] I. Safi, "Recent aspects concerning DC reactive magnetron sputtering of thin films: a review," *Surface and Coatings Technology*, vol. 127, pp. 203, 2000.

[15] M. Moradi, C. Nender, S. Berg, H.-O. Blom, A. Belkind, and Z. Orban, "Modeling of multicomponent reactive sputtering," *J. Vac Sci Technol. A*, vol. 9, pp. 619-24, 1991.

[16] P. Carlsson, C. Nender, H. Barankova, and S. Berg, "Reactive sputtering using two reactive gases, experiments and computer modeling," *J. Vac Sci Technol. A*, vol. 11, pp. 1534-9, 1993.

[17] D. Rosén, I. Katardjiev, S. Berg, and W. Moller, "TRIDYN Simulation of Target Poisoning in Reactive Sputtering," *Nucl. Instr. Meth.*, vol. 228, pp. 193-197, 2005.

[18] A. Pflug, B. Szyszka, V. Sittinger, and J. Niemann, "Process Simulation for Advanced Large Area Optical Coatings," presented at 46th Annual SVC Technical Conference, San Francisco, CA, 2003.

[19] Y. Matsuda, K. Otomo, and H. Fujiyama, "Quantitative modeling of reactive sputtering process for MgO thin film deposition," *Thin Solid Films*, vol. 390, pp. 59, 2001.

[20] K. Macak, T. Nyberg, P. Macak, M. Kharrazi Olsson, U. Helmersson, and S. Berg, "Modeling of the deposition of stoichiometric Al2O3 using nonarcing direct current magnetron sputtering," *J. Vac Sci Technol. A*, vol. 16, pp. 1286-92, 1998.

[21] I. Petrov, A. Myers, J. E. Greene, and J. R. Abelson, "Mass and energy resolved detection of ions and neutral sputtered species incident at the substrate during reactive magnetron sputtering of Ti in mixed $Ar+N_2$ mixtures," *Journal of Vacuum Science & Technology A (Vacuum, Surfaces, and Films)*, vol. 12, pp. 2846, 1994.

[22] C. R. Aita, "In situ sputter deposition discharge diagnostics for tailoring ceramic film growth," *Journal of Vacuum Science & Technology A: Vacuum, Surfaces, and Films*, vol. 16, pp. 1303, 1998.

[23] L. B. Jonsson, T. Nyberg, and S. Berg, "Dynamic simulations of pulsed reactive sputtering processes," *Journal of Vacuum Science and Technology, Part A: Vacuum, Surfaces and Films*, vol. 18, pp. 503, 2000.

[24] D. Rosén, O. Kappertz, T. Nyberg, I. Katardjiev, and S. Berg, "Complex Target Poisoning Effects in Reactive Sputtering," presented at AVS 51st National Symposium, Anaheim, California, USA, 2004.

[25] O. Kappertz, T. Nyberg, D. Rosén, I. Katardjiev, and S. Berg, "A Simplified Treatment of Target Implantation Effects in Reactive Sputtering," presented at The International Conference on Metalurgical Coatings and Thin Films, San Diego, California, USA, 2004.

[26] J. N. Avaritsiotis and C. D. Tsiogas, "A reactive sputtering process model for symmetrical planar diode systems.," *Thin Solid Films*, vol. 209, pp. 17-25, 1992.
[27] W. Eckstein, *Computer simulation of ion-solid interactions*. Berlin, Heidelberg: Springer-Verlag, 1991.
[28] J. P. Biersack and L. G. Haggmark, "A Monte Carlo Computer Program for the Transport of Energetic Ions in Amorphous Targets," *Nucl. Instr. Meth.*, vol. 174, pp. 257-269, 1980.
[29] W. Möller and W. Eckstein, "TRIDYN - A Trim Simulation Code Including Dynamic Composition Changes," *Nucl. Instr. Meth.*, vol. 230, pp. 814-818, 1983.
[30] W. Möller, W. Eckstein, and J. P. Biersack, "TRIDYN - Binary Collision Simulation of Atomic Collisions and Dynamic Composition Changes in Solids," *Comput. Phys. Commun.*, vol. 51, pp. 355-368, 1988.
[31] W. Eckstein and P. Biersack, "Computer Simulation of Two-Component Target Sputtering," *Appl. Phys. A: Solids Surf.*, vol. A 37, pp. 95-108, 1985.
[32] W. Möller and M. Posselt, *TRIDYN User Manual*, 2001.
[33] D. Rosén, "Defining the Surface Binding Energy in Dynamic Monte Carlo Simulation for Reactive Sputtering of Compounds," *To be published in Vacuum*.
[34] J. A. Thornton, "The microstructure of sputter-deposited coatings," *Journal of Vacuum Science & Technology A (Vacuum, Surfaces, and Films)*, vol. 4, pp. 3059, 1986.
[35] P. B. Barna and M. Adamik, "Fundamental structure forming phenomena of polycrystalline films and the structure zone models," *Thin Solid Films*, vol. 317, pp. 27, 1998.
[36] I. Petrov, P. B. Barna, L. Hultman, and J. E. Greene, "Microstructural evolution during film growth," *Journal of Vacuum Science and Technology A: Vacuum, Surfaces and Films*, vol. 21, pp. 117-128, 2003.
[37] J. E. Greene, S. A. Barnett, J. E. Sundgren, and A. Rockett, *Ion Beam Assisted Film Growth*. Amsterdam: Elsevier, 1988.
[38] K. M. Lakin, "A review of thin-film resonator technology," *IEEE Microwave Magazine*, vol. 4, pp. 61, 2003.
[39] R. C. Ruby, P. Bradley, Y. Oshmyansky, A. Chien, and J. D. Larson Iii, "Thin film bulk wave acoustic resonators (FBAR) for wireless applications," Atlanta, GA, 2001.
[40] S. Marksteiner, M. Handtmann, H. J. Timme, R. Aigner, R. Welzer, J. Portmann, and U. Bauernschmitt, "A miniature BAW duplexer using flip-chip on LTCC," Honolulu, HI, United States, 2003.
[41] H. P. Loebl, C. Metzmacher, D. N. Peligrad, R. Mauczok, M. Klee, W. Brand, R. F. Milsom, P. Lok, F. Van Straten, A. Tuinhout, and J. W. Lobeek, "Solidly mounted bulk acoustic wave filters for the GHz frequency range," Munich, Germany, 2002.

[42] D. Rosén, J. Bjurström, and i. Katardjiev, "Suppression of Spurious Lateral Modes in Thickness-Excited FBAR Resonators," *IEEE Trans. Ultrason. Ferroelect. Freq. Contr.*, vol. 52, 2005.
[43] "Bulk acoustic wave resonator with improved lateral mode suppression." European Patent, Application No. 00102624.4.: Agilent Technologies Inc.
[44] J. Kaitila, M. Ylilammi, J. Ella, and R. Aigner, "Spurious resonance free bulk acoustic wave resonators," Honolulu, HI, United States, 2003.
[45] J. Kaitila, J. Ella, and M. Ylilammi, "Resonator Structure and Filter Comprising Such a Resonator Structure." Patent Application No. WO2001006647 Al.
[46] K. M. Lakin, "Bulk acoustic wave coupled resonator filters," New Orleans, LA, United States, 2002.
[47] R. Aigner, "MEMS in RF-filter applications: thin film bulk-acoustic-wave technology," *Sensors Update*, vol. 12, pp. 175 - 210, 2003.
[48] T. Makkonen, A. Holappa, and M. M. Salomaa, "3D FEM modeling of composite BAW resonators," San Juan, 2000.
[49] T. Makkonen, A. Holappa, J. Ella, and M. M. Salomaa, "Finite element simulations of thin-film composite BAW resonators," *IEEE Transactions on Ultrasonics, Ferroelectrics, and Frequency Control*, vol. 48, pp. 1241, 2001.
[50] H. Nowotny and E. Benes, "General one-dimensional treatment of the layered piezoelectric resonator with two electrodes," *Journal of the Acoustical Society of America*, vol. 82, pp. 513, 1987.
[51] H. Nowotny, E. Benes, and M. Schmid, "Layered piezoelectric resonators with an arbitrary number of electrodes (general one-dimensional treatment)," *Journal of the Acoustical Society of America*, vol. 90, pp. 1238, 1991.
[52] J. F. Rosenbaum, *Bulk Acoustic Wave Theory and Devices*. Norwood, USA, 1988.
[53] J. D. Larson III, P. D. Bradley, S. Wartenberg, and R. C. Ruby, "Modified Butterworth-Van Dyke circuit for FBAR resonators and automated measurement system," San Juan, 2000.
[54] G. F. Iriarte, F. Engelmark, I. V. Katardjiev, V. Plessky, and V. Yantchev, "SAW COM-parameter extraction in AlN/diamond layered structures," *IEEE Transactions on Ultrasonics, Ferroelectrics, and Frequency Control*, vol. 50, pp. 1542, 2003.
[55] J. Bjurstrom, D. Rosen, I. Katardjiev, V. M. Yanchev, and I. Petrov, "Dependence of the electromechanical coupling on the degree of orientation of c-textured thin AlN films," *IEEE Transactions on Ultrasonics, Ferroelectrics, and Frequency Control*, vol. 51, pp. 1347, 2004.
[56] I. Katardjiev, J. Bjurström, and G. Wingqvist, "Production of polycrystalline films for shear mode piezoelectric thin film resonators." Swedish patent application #0500647-3, 2005.

[57] J. Bjurstrom, I. Katardjiev, and V. Yantchev, "Lateral-field-excited thin-film Lamb wave resonator," *Applied Physics Letters*, vol. 86, pp. 154103, 2005.

Acta Universitatis Upsaliensis

Digital Comprehensive Summaries of Uppsala Dissertations from the Faculty of Science and Technology 142

Editor: The Dean of the Faculty of Science and Technology

A doctoral dissertation from the Faculty of Science and Technology, Uppsala University, is usually a summary of a number of papers. A few copies of the complete dissertation are kept at major Swedish research libraries, while the summary alone is distributed internationally through the series Digital Comprehensive Summaries of Uppsala Dissertations from the Faculty of Science and Technology. (Prior to January, 2005, the series was published under the title "Comprehensive Summaries of Uppsala Dissertations from the Faculty of Science and Technology".)

Distribution: publications.uu.se
urn:nbn:se:uu:diva-6320

ACTA
UNIVERSITATIS
UPSALIENSIS
UPPSALA
2006